



Vattenfall Wind Power Ltd

Thanet Extension Offshore Wind Farm

**Annex 2-3: Geophysical Investigation Report
2 of 3 - Geophysical Site Survey**

June, 2017, Revision A

Document Reference: 6.4.2.3

Pursuant to: APFP Reg. 5(2)(a)

Vattenfall Wind Power Ltd

Thanet Extension Offshore Wind Farm

Annex 2-3: Geophysical Investigation Report 2 of 3 - Geophysical Site Survey

June, 2018

Drafted By:	Fugro Group
Approved By:	Helen Jameson
Date of Approval	June 2018
Revision	A

Copyright © 2018 Vattenfall Wind Power Ltd

All pre-existing rights reserved

Fugro

Thanet Extension Offshore Wind Farm

United Kingdom Continental Shelf, North Sea

**Report 1 of 3:
Geophysical Investigation Report**

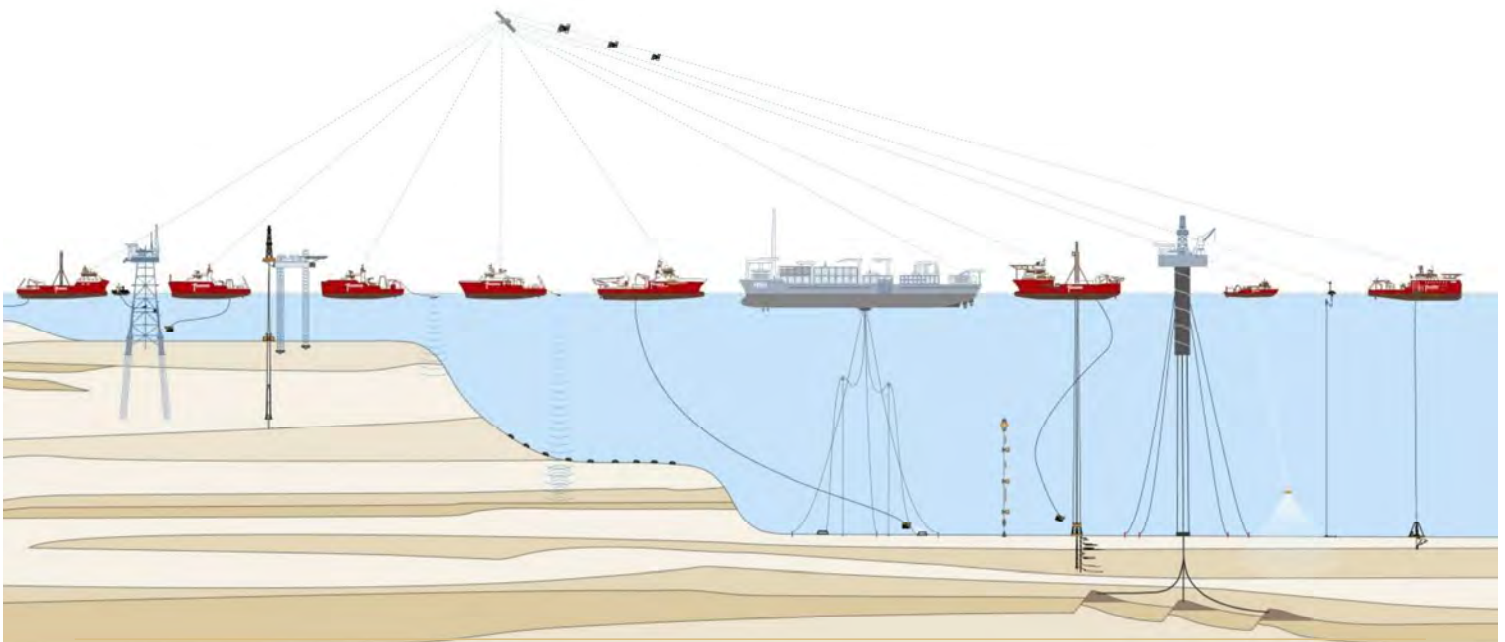
Volume 2 of 3:
Geophysical Site Survey

July to September 2016
Fugro (FSBV) Report No.: GE051-R1

Vattenfall Wind Power Ltd.



Revision 0





Prepared by: Fugro Survey B.V.
12 Veurse Achterweg
P.O. Box 128
2260 AC Leidschendam
The Netherlands
Phone +31 70 3111800
Fax +31 70 3111838
E-mail: FSBVinfo@fugro.com
Trade Register Nr: 34070322 / VAT Nr:005621409B11

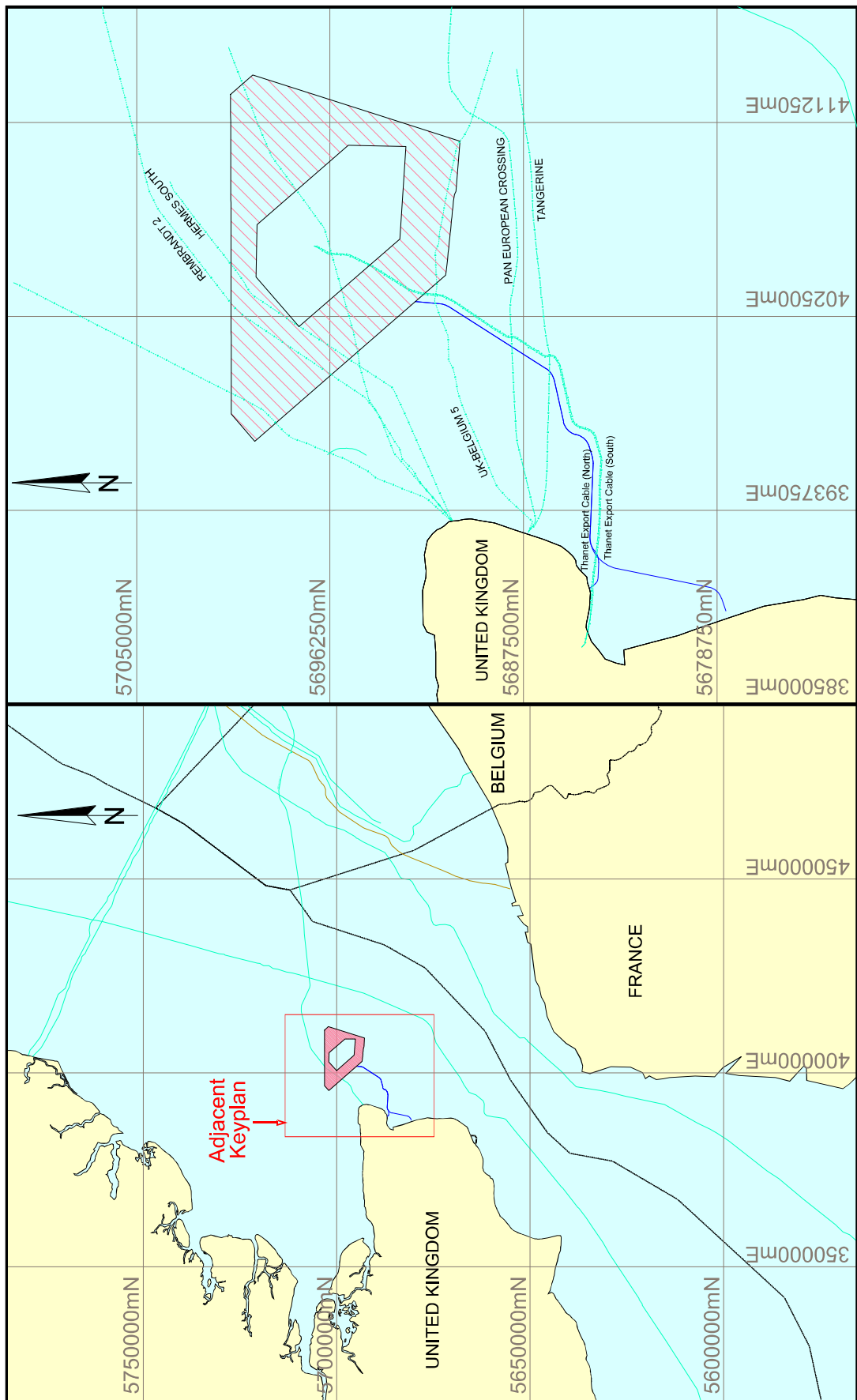
Prepared for: Vattenfall Wind Power Ltd
St Andrew House, Haugh Lane, Hexham
NE45 3QQ
Northumberland
United Kingdom

0	Final Issue	V. Minorenti	J. Chisholm	P.P. Lebbink	03 April 2017
1	Issue for Approval	M. van der Linde W. Teck Wu C. McGovern	V. Minorenti	P.P. Lebbink	25 November 2016
Rev	Description	Prepared	Checked	Approved	Date

REPORT AMENDMENT SHEET

Issue No.	Report section	Page No.	Table No.	Figure No.	Description
0	1.1	1	-	-	Text amended
0	1.3	3	-	-	"European Terrestrial System 1980" replaced with "... 1989"
0	2.3	9	-	-	Text amended
0	2.3	9	-	2.4	Figure replaced
0	2.3	10	-	-	"luff-faces" replaced with "stoss side"
0	2.3	14	-	2.5	Figure replaced
0	2.7.1	21	-	2.8	Legend added to figure
0	2.7.2	33	-	-	Text reworked (par no. 2)
0	2.8.4	39	-	-	Text reworked (par no. 1)
0	3.2.3	43	-	-	Typo corrected. Sentence regarding gridding artefacts amended
0	3.2.3	44	-	3.3	Profile in image replaced in red
0	3.5	46	-	-	Typo corrected
0	3.5	46	-	-	Added clarification on the source of noise in the magnetometer data
0	3.7.4	49	-	-	Text amended

VATTENFALL WIND POWER LTD.
 THANET EXTENSION OFFSHORE WIND FARM GEOPHYSICAL INVESTIGATION
 GEOPHYSICAL SITE SURVEY



KEYPLAN

EXECUTIVE SUMMARY

Thanet Extension	
Introduction	
Survey Dates:	July to September 2016
Equipment (Geophysical):	Sidescan sonar (SSS), single beam echo sounder (SBES), multibeam echo sounder (MBES), pinger (SBP), ultra high resolution (UHR) multichannel and magnetometer (MAG).
Coordinate System:	Datum: European Terrestrial Reference System 1989 (ETRS89) Projection: UTM Zone 31N, CM 3°E
Bathymetry	
<p>Water depths throughout the extended site range between approximately 11.5 and 49.0 m below LAT. As a general trend, shallower sections occur in the west and south-west part of the survey area while the seabed deepens towards the north-east and, especially, the east flank.</p> <p>A notable feature that marks an exception to this trend is a reef complex (Drill Stone Reef) in the north-east sector, where water depths decrease to as low as 12.0 m.</p>	
Seabed Features	
<p>Subaqueous dunes of different scales are highly abundant indicating a complex tidal and bottom-current regime.</p> <p>Generally, the seabed is characterised by SAND- and GRAVEL-type sediments with silty or clayey components in certain areas and coarse sand-sized to gravel-sized SHELL fragments.</p>	
Geology	
<p>The shallow sub-surface geological conditions within the survey area have been interpreted based on SBP and multichannel UHR sparker/air gun data and information from BGS standard geological maps (Ref. 8). The limit of interpretation of the UHR data to achieve satisfactory results was set at a depth of 250 m below seabed. Eight (8) seismic units were identified across the survey area including formations from the Holocene age to the late Cretaceous.</p>	
Seabed and Sub-seabed Hazards	
Wrecks	
<p>Nine (9) wrecks were observed within the TEOW. Three (3) additional charted wrecks were not found during this survey.</p>	
Cables	
<p>A total of seven (7) cables cross the TEOW based on the ENC and Admiralty charts. Two (2) cables were not detected by any geophysical survey equipment.</p>	
Thanet Export Cable (North)	Up to 3 m offset with respect to the database position
Thanet Export Cable (South)	Up to 5 m offset with respect to the database position
Rembrandt 2	Up to 33 m offset with respect to the database position
Hermes South	Up to 5 m offset with respect to the database position
UK-Belgium 5	Not observed
Unknown 1	Not observed
Unknown 2	Up to 200 m south of the database position
Seabed Geohazards	
Seabed gradients	Local seabed gradients in the north-east sector often exceed 20 degrees and reach a maximum of about 32 degrees.
Other contacts	Numerous suspected debris and unknown magnetometer contacts were observed scattered across the TEOW.
Sub-seabed Geohazards	
Palaeochannel Infills	Buried channels have been identified across the Unit B, Unit C and Unit E with variable orientation and depths.



Coarse Sediments / GRAVEL Layers / Boulders	Patches of hard layers / GRAVEL layers were identified in the west and east portions of the site within Unit C at variable depths.
Peat or Organic Sand / Clay Layers and/ or Shallow Biogenic Gas Accumulations	Most of the interpreted shallow gas is associated with shallow channels. Possible peat layers or organic sand / clay are also found along the base of Unit B.
Faulting	
Sedimentary units are moderately faulted due to the uplift events and differential compactions.	



DOCUMENT ARRANGEMENT

- REPORT 1: GEOPHYSICAL INVESTIGATION REPORT**
VOLUME 1: OPERATIONS & CALIBRATIONS
VOLUME 2: GEOPHYSICAL SITE SURVEY
VOLUME 3: GEOPHYSICAL ROUTE SURVEY
- REPORT 2: GEOTECHNICAL INVESTIGATION REPORT
- REPORT 3: ENVIRONMENTAL INVESTIGATION REPORT

CONTENTS

1.	INTRODUCTION AND SCOPE OF WORK	1
1.1	General	1
1.2	Purpose of Work	2
1.3	Geodetic Parameters	3
2.	SURVEY RESULTS	4
2.1	Bathymetry	4
2.2	Sedimentary Bedforms	5
2.3	Seabed and Sediment Classification	9
2.4	Seabed Contacts	15
2.5	Other Contacts	17
2.6	Regional Geology	18
2.7	Local Geology	21
2.7.1	Overview	21
2.7.2	Local Stratigraphy	24
2.8	Installation Constraints	36
2.8.1	Palaeochannel Infill	36
2.8.2	Coarser Sediments / GRAVEL Layers / Boulders	37
2.8.3	Peat or Organic Sand / Clay Layers and/ or Shallow Biogenic Gas Accumulations	37
2.8.4	Faulting	39
3.	DATA REDUCTION AND PROCESSING	40
3.1	Positioning and Navigation	40
3.2	Multibeam Echo Sounder	40
3.2.1	Bathymetry Processing Workflow	40
3.2.2	Bathymetry assembling	41
3.2.3	Sediment movements	42
3.2.4	Small vertical mismatches	44
3.3	Backscatter Data	44
3.4	Sidescan Sonar	45
3.5	Magnetometer	46
3.6	Sub-bottom Profiler	47
3.7	Data Interpretation	48
3.7.1	Bathymetry Data Interpretation	48
3.7.2	Sidescan Sonar Data Interpretation	48
3.7.3	Magnetometer Data Interpretation	48
3.7.4	Seismic Data Interpretation and Gridding Methodology	48
4.	REFERENCES	51

APPENDICES

- A. TRACK CHARTS
- B. BATHYMETRY CHART
- C. SEABED AND SEDIMENT CLASSIFICATION CHARTS
- D. CONTACT CHARTS
- E. GEOLOGICAL CHARTS
- F. GEOHAZARD CHART
- G. UHR SEISMIC PROCESSING REPORT

TABLES

Table 1.1: Project geodetic and projection parameters	3
Table 2.1: Classification scheme for seabed bedforms (Ref. 1)	5
Table 2.2: List and Description of Bedforms within the Survey Area	7
Table 2.3: Data Example for Outcrops and the Reef	11
Table 2.4: Description and Data Examples of Natural Seabed Features	12
Table 2.5: Overview and Data Examples of Anthropogenic Seabed Contacts	15
Table 2.6: Cables crossing TEOW	16
Table 2.7: As-found wreck locations across the Thanet Extension Site	17
Table 2.8: Summary table for SSS and magnetometer contacts	18
Table 2.9: Overview of the interpreted seismic units	22
Table 3.1: Caris HIPS & SIPS bathymetry workflow	40
Table 3.2: Settings and sequence of magnetometer data filters	46
Table 3.3: Settings and sequence of magnetometer data filters for geological assessment	47
Table 3.4: Gridding and contouring methodology and parameters	50

FIGURES

Figure 2.1: Bathymetric overview of the extended Thanet site. Existing MBES data for the original site is presented as a slightly bleached out area.	4
Figure 2.2: Seabed gradients calculated from MBES data	5
Figure 2.3: First order description parameters of (a) 2D and (b) 3D seabed dunes (Ref. 1 modified)	6
Figure 2.4: Multibeam backscatter data for the Thanet Extension Site.	9
Figure 2.5: Comparison of bathymetry data from 2012 and 2016 over very large dunes and ridges (red profile: 2012 green profile: 2016)	14
Figure 2.6: Cross section showing the Late Cretaceous to Quaternary sediments, 5 km from the survey area (modified from ref. 8)	19
Figure 2.7: Overview of the glacial extents in the North Sea Basin during the Holocene (modified from ref. 9)	20
Figure 2.8: Survey area plotted on geologic chart (modified from ref. 8)	21
Figure 2.9: Unit B incising into underlying deposits	24



Figure 2.10: Overview of the full geologic section within the survey area	27
Figure 2.11: Fault structures within Unit D	29
Figure 2.12: Parallel bedding within Unit D	30
Figure 2.13: Parallel bedding within Unit E and the erosional surface H20	32
Figure 2.14: Units E, F, G and H including fault structures within Unit F, G and H and a channel structure within Unit E	35
Figure 2.15: Possible hard/coarse sediment layer	38
Figure 3.1: Thanet Extension block definition	42
Figure 3.2: Observed sediment movement in survey block overlapping areas	43
Figure 3.3: Ripple migrations between block 1 and block 2a	44
Figure 3.4: Small dB offsets in Backscatter on Block 1	45
Figure 3.5: Backscatter anomaly in nadir region on sand ripple crest	45

LIST OF CHARTS

Appendix	Drawing	Chart Name	Scale	Enclosure
A	Track Charts			
	Track Plot Magnetometer	GE051_TE_TRACK-MAG_NU_10K	1 : 10,000	01-03
	Track Plot Multibeam	GE051_TE_TRACK-MBE_NU_10K	1 : 10,000	04-06
	Track Plot Sub-bottom Profiler	GE051_TE_TRACK-SBP_NU_10K	1 : 10,000	07-09
	Track Plot Sidescan Sonar	GE051_TE_TRACK-SSS_NU_10K	1 : 10,000	10-12
	Track Plot UHR Sparker	GE051_TE_TRACK-UHR_NU_10K	1 : 10,000	13-15
B	Bathymetry Chart			
	Shaded Relief Bathymetry Chart	GE051_TE_BATHY_NU_10K	1 : 10,000	16-18
C	Seabed and Sediment Classification Charts			
	Seabed Classification Chart	GE051_TE_SBF_NU_E_10K	1 : 10,000	19-21
	Sediment Classification Chart	GE051_TE_SEDIMENT_NU_10K	1 : 10,000	22-24
D	Contact Charts			
	Contacts and Sidescan Sonar Mosaic Chart	GE051_TE_CONTACTS_NU_10K	1 : 10,000	25-27
	Contacts and Magnetometer Ribbon Plot Chart	GE051_TE_RIBBON_NU_10K	1 : 10,000	28-30
E	Geological Charts			
	Horizon H01_bLAT	GE051_TE_H01_bLAT_NU_10K	1 : 10,000	31-33
	Horizon H01_bsb	GE051_TE_H01_bsb_NU_10K	1 : 10,000	34-36
	Horizon H02_bLAT	GE051_TE_H02_bLAT_NU_10K	1 : 10,000	37-39
	Horizon H02_bsb	GE051_TE_H02_bsb_NU_10K	1 : 10,000	40-42
	Horizon H09_bLAT	GE051_TE_H09_bLAT_NU_10K	1 : 10,000	43-45
	Horizon H09_bsb	GE051_TE_H09_bsb_NU_10K	1 : 10,000	46-48
	Horizon H10_bLAT	GE051_TE_H10_bLAT_NU_10K	1 : 10,000	49-51
	Horizon H10_bsb	GE051_TE_H10_bsb_NU_10K	1 : 10,000	52-54
	Horizon H20_bLAT	GE051_TE_H20_bLAT_NU_10K	1 : 10,000	55-57
	Horizon H20_bsb	GE051_TE_H20_bsb_NU_10K	1 : 10,000	58-60
	Horizon H30_bLAT	GE051_TE_H30_bLAT_NU_10K	1 : 10,000	61-63
	Horizon H30_bsb	GE051_TE_H30_bsb_NU_10K	1 : 10,000	64-66
	Horizon H40_bLAT	GE051_TE_H40_bLAT_NU_10K	1 : 10,000	67-69
	Horizon H40_bsb	GE051_TE_H40_bsb_NU_10K	1 : 10,000	70-72
F	Geohazard Chart			
	Geohazard Chart	GE051_TE_GEOHAZARD_NU_10K	1 : 10,000	73-75

ABBREVIATIONS

BGS	British Geological Survey
bLAT	below Lowest Astronomical Tide
bsb	below seabed
CM	Central Meridian
COG	Centre of Gravity
CPT	Cone Penetration Test
CRP	Common Reference Point
DGPS	Differential Global Positioning System
DTM	Digital Terrain Model
DTU13	Danish Technical University 2013
ENC	Electronical Nautical Chart
EPSG	European Petroleum Survey Group
ETRS89	European Terrestrial Reference System 1989
Fm	Formation
FSBV	Fugro Survey B.V.
GIS	Geographic Information Systems
GNSS	Global Navigation Satellite System
GPS	Global Positioning System
HIPS	Hydrographic Information Processing System
HVF	HIPS Vessel File
ITRF	International Terrestrial Reference Frame
LAT	Lowest Astronomical Tide
MAG	Magnetometer
MBBS	Multibeam Backscatter Sonar
MBES	Multibeam echo sounder
MV	Motor Vessel
QC	Quality Control
SBES	Single beam echo sounder
SBP	Sub-bottom profiler
SCS	Single channel seismic
SIPS	Sonar Information Processing System
SIS	Seafloor Information System
SSS	Sidescan sonar
TEOW	Thanet Extension Offshore Wind Farm
TPU	Total Propagated Uncertainty
TVG	Time variable gain
TWT	Two way travel (time)
UHR	Ultra High Resolution
UHRS	Ultra High Resolution Seismic
UKOOA	United Kingdom Offshore Operators Association
UTC	Coordinated Universal Time
UTM	Universal Transverse Mercator
VORF	Vertical Offshore Reference Frame
WGS84	World Geodetic System 1984

1. INTRODUCTION AND SCOPE OF WORK

1.1 General

Vattenfall Wind Power Ltd. contracted Fugro to perform a geophysical investigation to improve the bathymetrical, morphological and geological understanding of the Thanet Extension Offshore Wind Farm (TEOW), located north-east of Kent off the United Kingdom coast. Furthermore the geophysical results were used for UXO/obstructions clearance for the following geotechnical campaign. The results of the geotechnical campaign are integrated with the geophysical data to create a ground model. The ground model will serve as the base for the design and installation requirements.

Geophysical information for the Thanet Extension Offshore Windfarm are gathered and described in this report. Details of the survey operations, including vessels and equipment, and a discussion of data quality and accuracy, are included in the Operations and Calibrations Report (Report 1, Operations & Calibrations Report).

The geophysical survey was carried out using the survey vessels MV Fugro Pioneer for the site and the MV Discovery and Valkyrie for the cable route. The port in Great Yarmouth was the closest to the Thanet Extension Offshore Wind Farm area and it was used as main base for the survey operations.

The geophysical survey was carried out between July and September 2016.

Unless otherwise specified, all geographical and projection coordinates in the report and in the charts are based on local datum ETRS89. Projection coordinates are expressed in Universal Transverse Mercator (UTM) grid, Zone 31, Northern Hemisphere. The vertical datum is Lowest Astronomical Tide (LAT). The time standard is UTC +1.

The investigation provided geophysical bathymetric and shallow seismic data using the following equipment: sidescan sonar (SSS), magnetometer, multibeam and single beam echo sounder (MBES/SBES), sub-bottom profiler (SBP) and ultra-high resolution multichannel sparker (UHR).

This report focuses solely on the Thanet Extension site. A separate report is dedicated to the cable route (GE051 / R1 / Vol 3).

1.2 Purpose of Work

The general objectives for the site and cable route surveys were:

- Gather accurate bathymetric data and assess topography for areas with steep gradients and provide assessment of seabed movements;
- Collect sidescan sonar data and provide interpretation of seabed sediments and identification of any object on the seabed larger than 1 m;
- Collect sub-bottom profiler seismic data to assess variations in thickness of seabed sediments and shallow geology;
- Collect UHR seismic data and build a seismic stratigraphic model of the deeper geology (not for the export cable);
- Locate any structural complexities or geohazards within the shallow geological succession, such as faulting, accumulations of shallow gas, buried channels;
- Collect magnetometer data and include data in assessment of regional geology and provide identification of any magnetic anomalies;
- Gather seismic information about geotechnical borehole locations;
- Provide acoustic sediment type data to inform benthic surveys;
- Production of charts and maps suitable for use in GIS systems, including track plots, bathymetry, and seabed features with contacts, relative to LAT.

1.3 Geodetic Parameters

Unless otherwise specified, all geographical and projection coordinates in the report and in the charts are based on local datum European Terrestrial System 1989 (ETRS89). Projection coordinates are expressed in Universal Transverse Mercator (UTM) grid, Zone 31, Northern Hemisphere. The vertical datum is Lowest Astronomical Tide (LAT). The time standard is UTC +1.

Satellite navigation and positioning was operated in differential mode. DGPS geographical coordinates were based on datum World Geodetic System 1984. The UKOOA datum shift parameters were used for the transformation from WGS84 to the local coordinates in the ETRS89 datum. The geodetic parameters are detailed in Table 1.1.

Table 1.1: Project geodetic and projection parameters

Global Positioning System Geodetic Parameters ⁽¹⁾								
Datum:			ITRF2008 (WGS 84)					
Spheroid:			ITRF (WGS84)					
Semi major axis:			a = 6 378 137.000 m					
Inverse Flattening:			$1/f = 298.257223563$					
EPSG Code:			6326					
Local Datum Geodetic Parameters ⁽²⁾								
Datum:			European Terrestrial Reference System 1989 (ETRS89)					
Spheroid:			GRS80					
Semi major axis:			a = 6 378 137.000 m					
Inverse Flattening:			$1/f = 298.257222101$					
EPSG Code:			6258					
Datum Transformation Parameters ⁽³⁾ from WGS84 to ETRS89 for epoch 2016.647540984 (25 August 2016)								
Shift dX:	+0.05376	m	Rotation rX:	-0.002239	arcsec	Scale Factor:	+0.0026718	ppm
Shift dY:	+0.05096	m	Rotation rY:	-0.013547	arcsec			
Shift dZ:	-0.08847	m	Rotation rZ:	+0.021897	arcsec			
Project Projection Parameters								
Grid Projection:			Universal Transverse Mercator					
UTM Zone			31 Northern Hemisphere					
Central Meridian:			003° 00' 00.000" East					
Latitude of Origin:			00° 00' 00.000" North					
False Easting:			500 000 m					
False Northing:			0 m					
Scale factor on Central Meridian:			0.9996					
Units:			Metre					
EPSG Code:			25831					
Notes:								
1. Source: Starfix.NG. Starfix.NG determines the transformation parameters according to the Memo of C. Boucher and Z. Altamimi, dated 18 May 2011.								
2. This is the right-handed coordinate frame rotation convention used by the Fugro Starfix navigation software.								
3. The coordinate transformation parameters are the combined result of the 14 parameter transformation from ITRF2008 to ETRS89 and do take into account the yearly changes on the mentioned epoch.								
The WGS 84 realisation is nearly equal to the ITRF2008 on the above mentioned epoch. WGS 84 is maintained by the US Department of Defence to be nearly identical to ITRF2008.								

2. SURVEY RESULTS

2.1 Bathymetry

Water depths throughout the extended site range between approximately 11.5 m LAT and 49.0 m LAT. As a general trend, shallower sections occur in the west and south-west part of the survey area while the seabed deepens towards the north-east and, especially, the eastern flank. A notable feature that marks an exception to this trend is a reef complex in the north-east sector, where water depths decrease to as low as 12 m LAT. An overview of the survey area is provided in Figure 2.1. MBES data are presented in the **Bathymetry Chart**, Appendix B. The existing bathymetry dataset for the original site is presented as a reference as well as the newly acquired data for the north end of the cable route corridor.

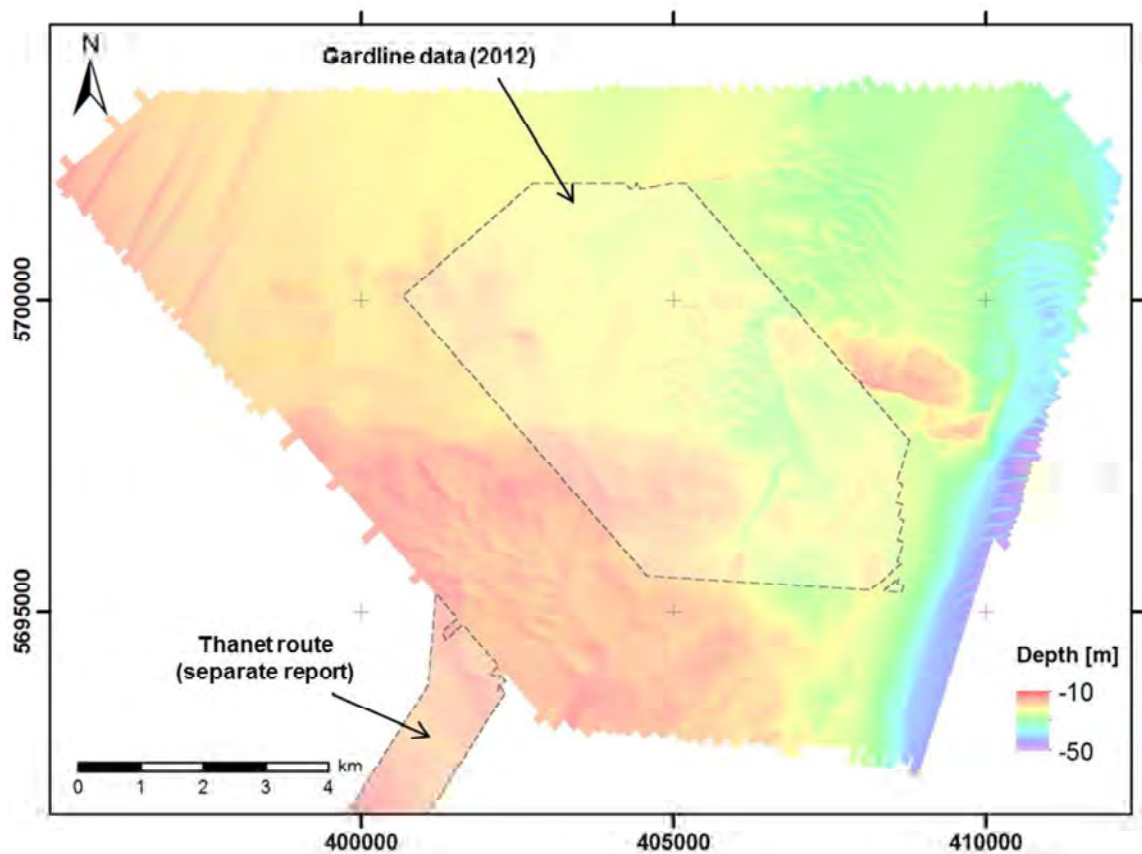


Figure 2.1: Bathymetric overview of the extended Thanet site. Existing MBES data for the original site is presented as a slightly bleached out area.

The majority of the seabed within the survey site is flat with gradients of less than five degrees. However, as shown in Figure 2.2, the north-east sector is characterised by the occurrence of very large subaqueous dunes which feature steep slope angles along flanks, in particular on the lee side. Local seabed gradients in these areas often exceed 20 degrees and reach a maximum of about 32 degrees. Isolated areas with seabed gradients larger than ten degrees, e.g. subaqueous dunes and sub- or outcropping seabed, are found throughout the whole survey site. Subaqueous dunes and other bedforms are described in detail in Section 2.2.

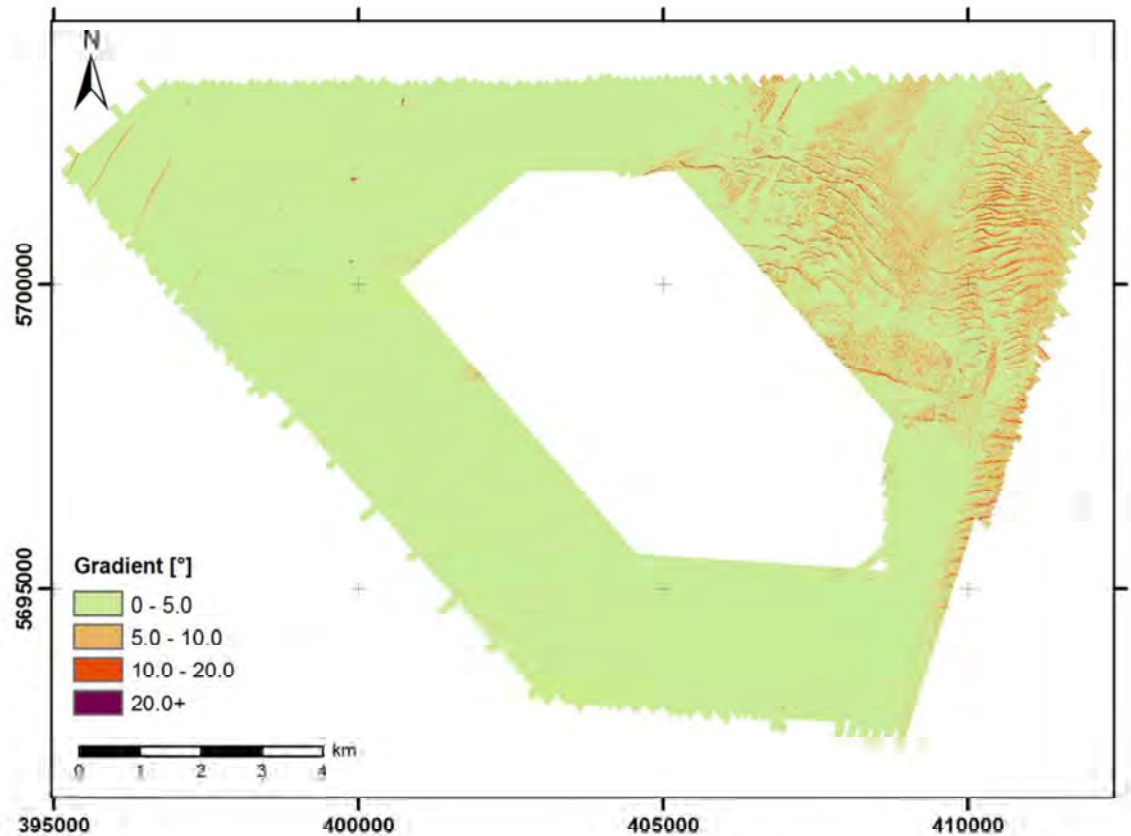


Figure 2.2: Seabed gradients calculated from MBES data

2.2 Sedimentary Bedforms

The sedimentary bedforms are presented in the **Seabed Features Charts**, Appendix C.

A large part of the seabed within the survey area is dominated by current-induced bedforms of various scales. According to Ashley et al. (2002, [Ref. 1](#)), current related seabed features such as ripples, sand waves and dunes can be jointly defined as dunes and classified in terms of height, spacing between features and shape (2D or 3D) as first order descriptors (Table 2.1 and Figure 2.3). This classification is used to describe the morphological features within the Thanet Extension site.

Table 2.1: Classification scheme for seabed bedforms ([Ref. 1](#))

General Class: Dune				
First Order Description				
Size				
Spacing	0.6-5 m	5-10 m	10-100 m	>100 m
Height	0.075-0.4 m	0.4-0.75 m	0.75-5 m	>5 m
Term	<i>small</i>	<i>medium</i>	<i>large</i>	<i>very large</i>
Shape				
2D	Straight-crested, little or no scour in trough			
3D	Sinuous, catenary or linguoid/lunate crested, deep scour in trough			
Second Order description				

Superposition	
Simple	No bedforms superimposed
Compound	Smaller bedforms superimposed

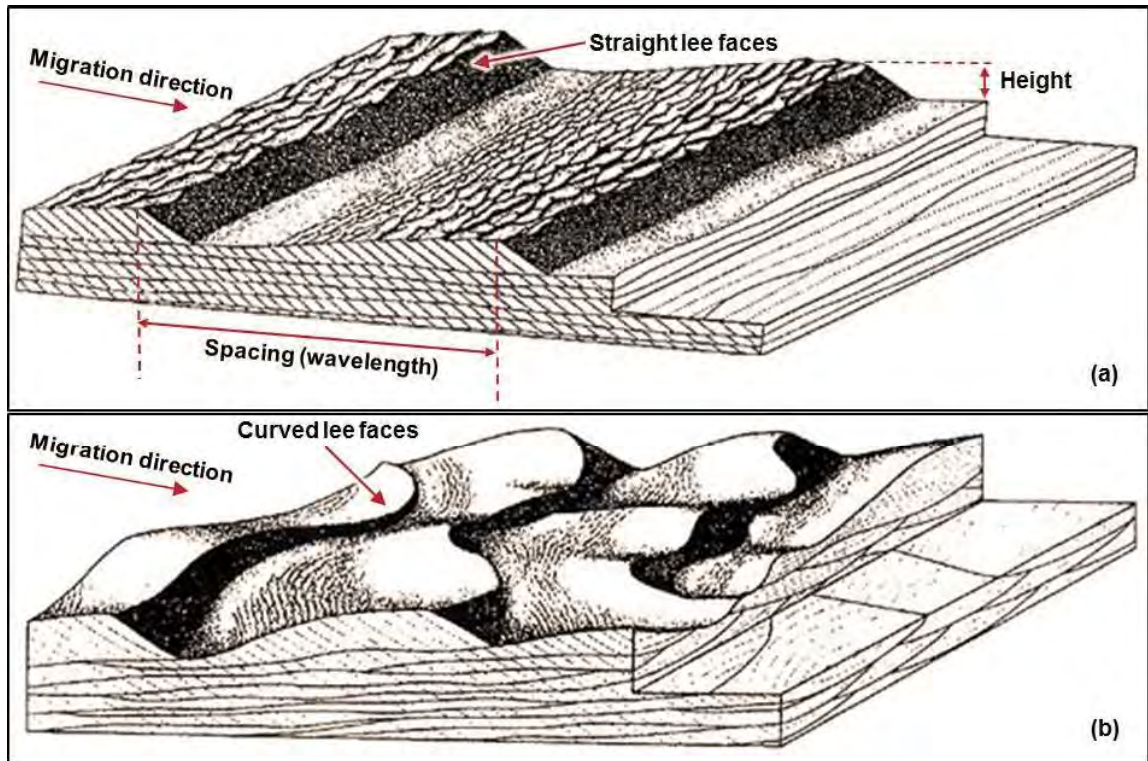


Figure 2.3: First order description parameters of (a) 2D and (b) 3D seabed dunes ([Ref. 1](#) modified)

The morphology, distribution and orientation of these dunes are an indicator for large sediment transport and current direction. Statistical analysis and modelling of sand dune mobility (e.g. [Ref. 2](#) and [Ref. 3](#)) shows that they typically migrate in the range of several metres per year. The high seabed gradients on the lee side of the dunes are identified as seabed hazards.

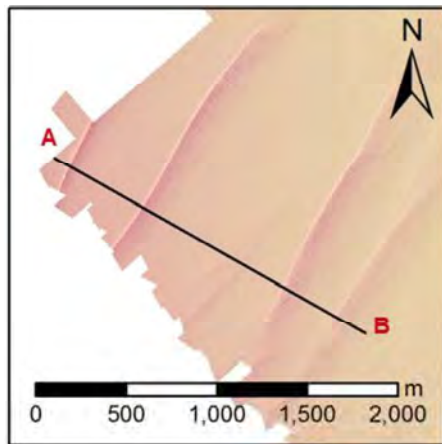
Subaqueous dunes of different scales are highly abundant, indicating a complex tidal and bottom-current regime. Table 2.2 provides data examples with description and classification of these bedforms.

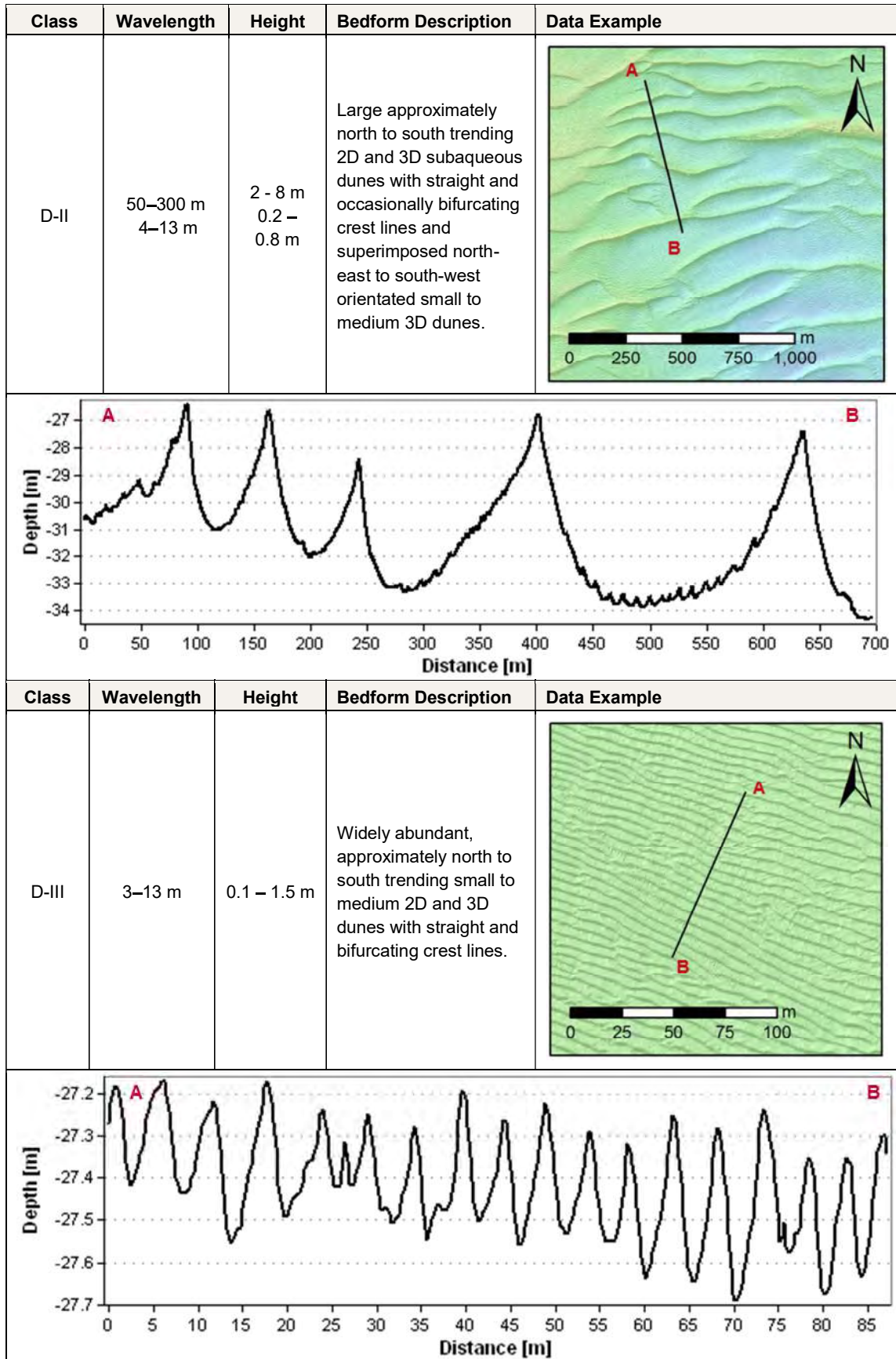
Several very large subaqueous 2D compound dunes with 300 to 600 m spacing and a height of about 4 to 6 m, categorised as class D-I, are found in the north-west corner of the survey site and suggest a low to moderate current (0.5 to 1.0 m/s, Stow et al, 2009, [Ref. 4](#)) in north-west direction. North-north-west to south-south-east (about 50° offset) running small to medium dunes (class D-III) superimpose on the crests, providing evidence of a second current direction, e.g. tidal and bottom currents. Further patches of small to medium dunes are identified in the troughs, which have the same orientation as the underlying structure. The crests of the very large dunes appear wide and flat but steepen towards the north-west.

The north-east sector is characterised by a high abundance of large to very large 2D and 3D subaqueous compound dunes, but these differ from the previously described ones in dimension, shape, orientation and superposition and are referred to in Table 2.2 as class D-II. Their wavelength is significantly shorter, usually between 100 and 250 m, with a few larger scattered dunes, and the crests are both higher and steeper. Where crest lines bifurcate, the wavelength may decrease to a few tens of metres. As illustrated in Figure 2.2 the orientation varies between north-north-west to south-south-east and north-east to south-west affected by the surrounding seabed morphology. Apart from the crests, the class I dunes are almost entirely superimposed by small to medium dunes (class D-III).

Approximately one third of the whole survey site is covered by small to medium subaqueous 2D and 3D dunes, either as superimposing or sole bedform. Apart from those described in relation with class D-I dunes, these dunes run in southerly directions. Their wavelength ranges from three to more than ten metres and their height from a decimetre to more than a metre. In Table 2.2 these are referred to as class D-III.

Table 2.2: List and Description of Bedforms within the Survey Area

Class	Wavelength	Height	Bedform Description	Data Example
D-I	300 - 600 m 4 - 8 m	2 - 3 m 0.1 - 0.4 m	Very large south-east to north-west trending, subaqueous 2D dunes with crests superimposed by small to medium dunes, straight crest lines and partial small to medium dune formations within troughs. Dunes on crests are north-north-west to south-south-east orientated	 <p>The 'Data Example' column for Class D-I contains two visualizations. The top visualization is a map showing a large, elongated, and slightly curved bedform area. A line segment labeled 'A' to 'B' indicates a cross-section line. A scale bar at the bottom ranges from 0 to 2,000 meters. A north arrow is in the top right corner. The bottom visualization is a bathymetric profile along the line A-B. The y-axis is 'Depth [m]' ranging from -13 to -17. The x-axis is 'Distance [m]' ranging from 0 to 2,000. The profile shows a series of large, rounded peaks (dunes) with smaller, sharper peaks (crests) superimposed on them. Two specific features are highlighted with red boxes: one at approximately 1,000m distance and another at approximately 1,500m distance. A red arrow points from the first box to the second.</p>



2.3 Seabed and Sediment Classification

Seabed feature and sediment classification is presented in the **Seabed Classification Charts and Sediment Classification Charts**, Appendix C.

A general classification of the seabed sediment is conducted primarily based on multibeam backscatter and sidescan sonar data. The backscatter mosaic for the whole site is shown in Figure 2.4 overlaid with sedimentological analyses of the environmental campaign added. As a rule of thumb, high backscatter strength (dark grey) corresponds with coarser sediments whereas low backscatter (light grey) indicates finer grain sizes. However, apart from seabed type, backscatter strength is also affected by, among others, incident angle, water depth and shallow geological condition. Hence, variations in intensity within one sediment type can occur across the site.

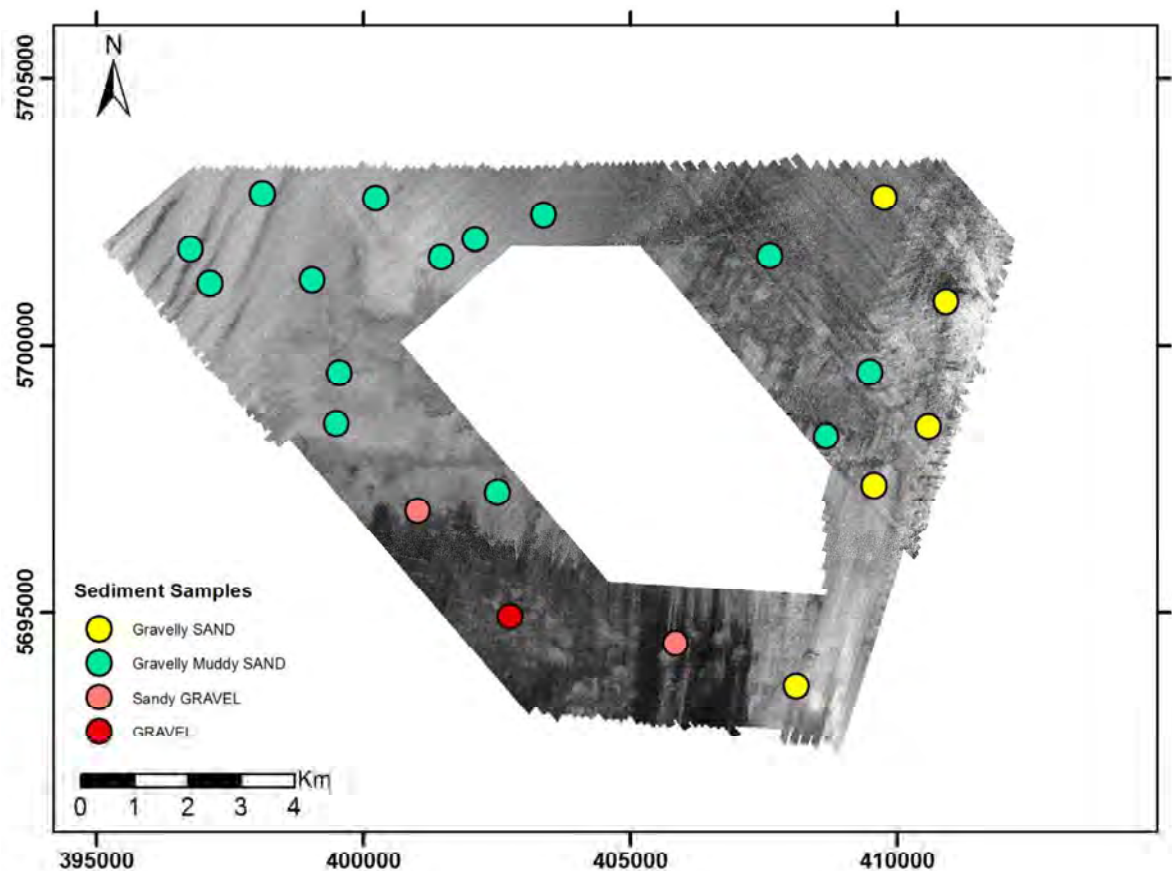


Figure 2.4: Multibeam backscatter data for the Thanet Extension Site.

Generally, the seabed is characterised by SAND- and GRAVEL-type sediments with silty or clayey components in certain areas and coarse sand-sized to gravel-sized shell fragments. For charting, sediment types are summarised into four categories, namely clayey or silty SAND, (fine to coarse) SAND, gravelly SAND and sandy GRAVEL and supplemented by two more additional categories for outcrops and reefs.

The north-west of the survey site features mostly (clayey) fine to medium SAND and sandy gravelly patches on the stoss-sides of the very large class dunes. Closer to the existing site, sub-surface unit C

is exposed in several spots resulting in an irregular seabed with numerous cobbles, boulders and boulder clusters. A data example of these areas is provided in Table 2.3.

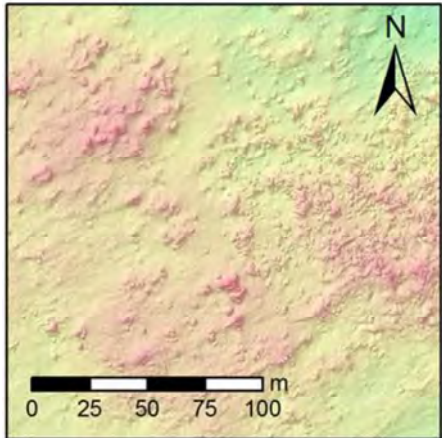
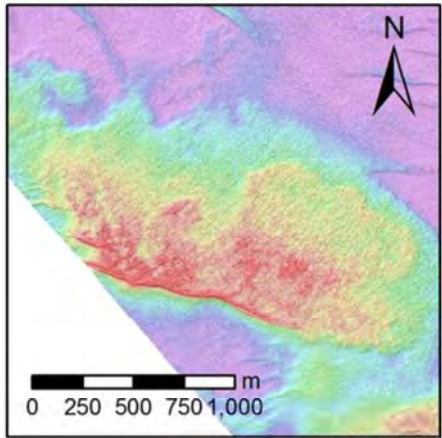
In the north and east, the majority of the seabed is covered by fine to coarse SAND with varying proportions of each constituent, which leads to many small-scale changes in backscatter intensity. The light-grey and dark-grey patches in Figure 2.4 represent pockets of clayey/silty and gravelly SAND, respectively. The aforementioned reef is located in the east, close to the existing site boundary.

A significant change in backscatter strength is noted in the south and south-west which is interpreted to be the result of multiple factors. Firstly, with water depths less than 20 m this area marks the shallowest section of the survey site. This results in less signal attenuation in the water column and, thus, a stronger base return. Secondly, the underlying chalk layer comes close to the seabed – locally outcropping - leaving only a few decimetres of loose sediments. Thin veneers of sediments are penetrated by the sonar, which further contributes to higher intensity levels. Thirdly and lastly, the sediment composition changes to mostly sandy GRAVEL and gravelly SAND with only a few minor pockets of medium to coarse SAND. While the SBP data do not confirm the abundance of a sediment layer on top of the chalk, variations of backscatter strength, the existence of north to south orientated sand ribbons visible in backscatter and sidescan sonar data, and one sediment sample in the area indicate a decimetre of loose sediments on the surface.

Outcrops present at the surface expressed the underlying sub-surface unit C and E (further discussed in section 2.7) with no or negligible sediment cover. Their spatial distribution is limited to areas in the north-west and smaller patches in the south section as described above.

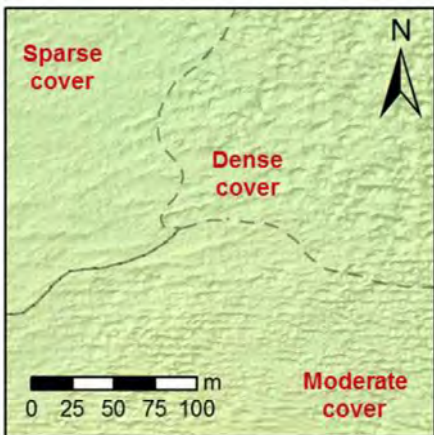
A major reef structure (Drill Stone Reef) presumably formed by *S. spinulosa* exists in the north-east of the survey area. The reef stretches over approximately 3.5 km in west-north-west to east-south-east direction with a maximum width of approximately 1.3 km including a slightly detached part in the south-east. Its south edge is marked by a relatively sharp and steep decline of up to 30 degrees with water depths decreasing from about 13 m to about 23 m over a distance of approximately 100 m. An extract from bathymetry data of the reef area is shown in Table 2.3.

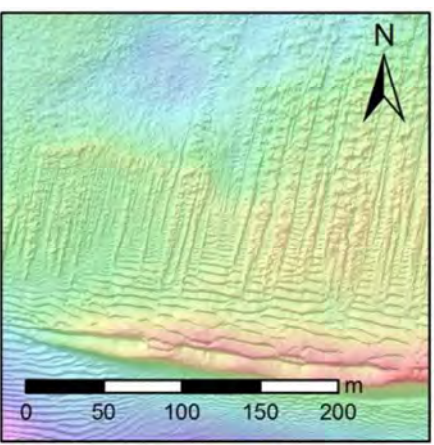
Table 2.3: Data Example for Outcrops and the Reef

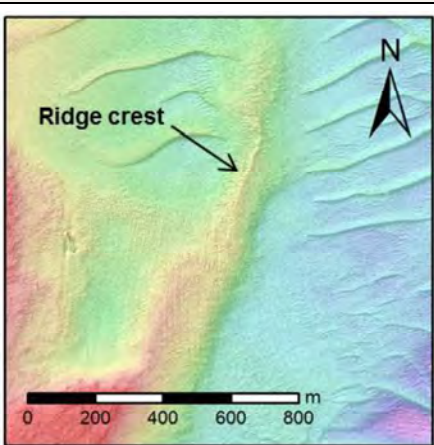
Seabed Feature	Dimension & Description	Data Example
Outcrop	Highly irregular seabed, outcropping and subcropping of the underlying unit C. Plenty of scattered boulders and boulder clusters resulting in chaotic undulations of up to one metre. The outcrops as a whole are elevated for up to several metres compared to surrounding seabed.	
Reef	A reef complex (Drill Stone Reef) formed by <i>Sabellaria spinulosa</i> . It extends over several kilometres and marks an elevation of approximately ten metres compared to the surrounding seabed.	

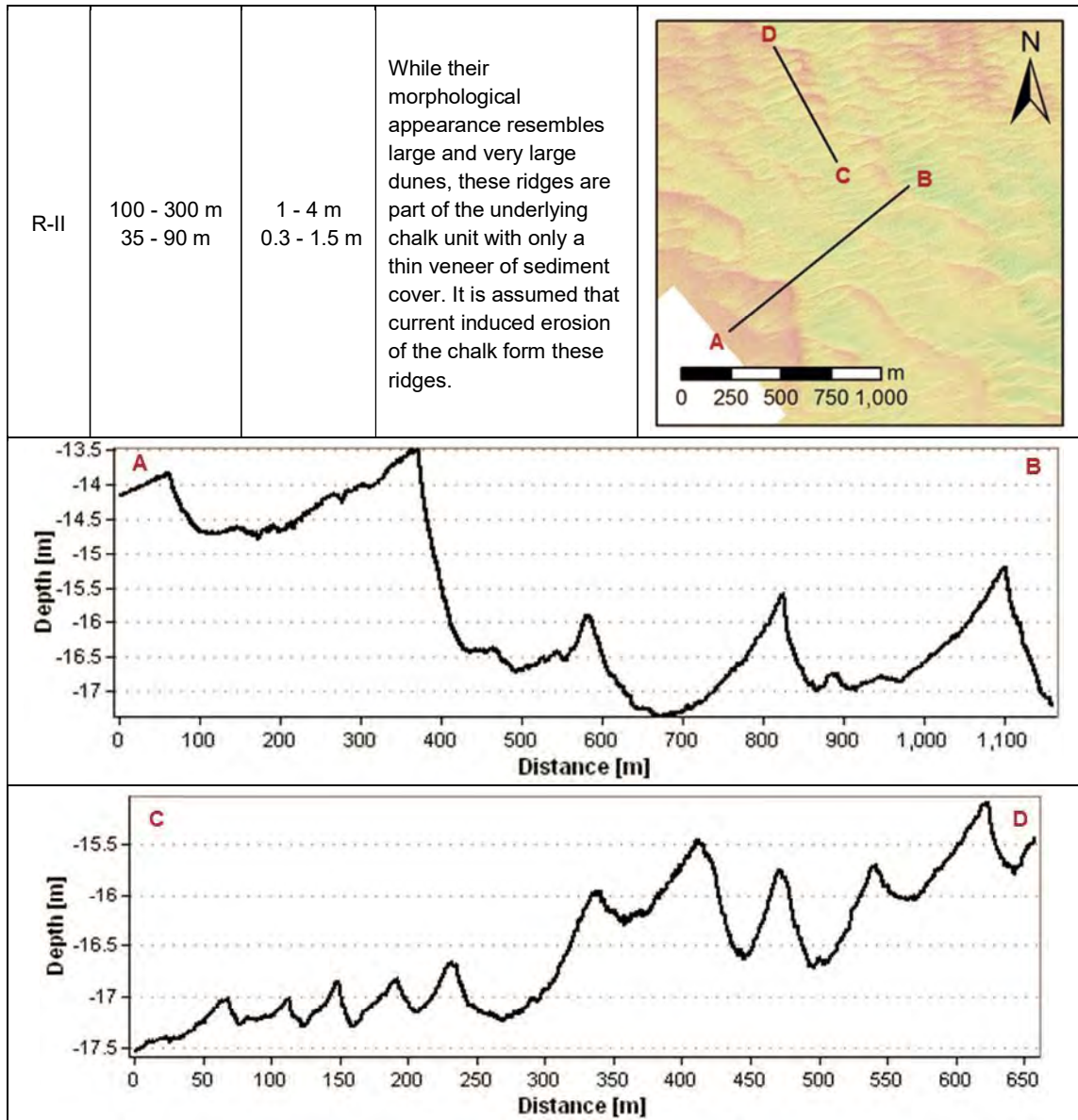
In the north-east sector of the survey site, areas of hummocky or rugged seabed are identified, which usually coincide with sections where sub-surface unit C comes close to the seabed and is only covered by a thin veneer of mobile sediments. Based on findings by Pearce et al (2014, [Ref. 5](#)) and Seiderer ([Ref. 6](#)), these areas are interpreted as *Sabellaria spinulosa* cover – a small tube-dwelling polychaete worm that is able to form reef structures given the right environmental conditions. Thereby, the acoustic signature from MBES, MBBS and SSS data gives insight into the density of *S. spinulosa* population. Taking into account ground-truthing samples from the aforementioned studies (photographs) and relating those to the newly acquired geophysical data, three categories are established distinguishing between sparse, moderate and dense coverage depending on the degree of seabed ruggedness. Table 2.4 provides an MBES data example showing the difference between spatial coverage. An environmental survey is currently being conducted and its results will give further insight into the benthic life in this area.

Table 2.4: Description and Data Examples of Natural Seabed Features

Class	Wavelength	Height	Bedform Description	Data Example
Sabellaria	n/a	Max. 1.5 m	Areas of hummocky or rugged seabed interpreted as cover of <i>Sabellaria spinulosa</i> . Categorized into sparse, moderate and dense coverage.	

Seabed Feature	Dimension & Description	Data Example
Seabed lineation	<p>Seabed lineations, also known as seabed scours or (longitudinal) furrows are found in three areas: at the east and west side of the reef complex and in the south-south-east. They usually extend over several hundreds of metres in north-south direction with widths of 5 to 12 m and heights between 0.1 and 0.6 m. Their presence appears to be limited to areas of elevated seabed. All lineations are assumed to be associated with the same geological process.</p> <p>In literature, similar features, though of larger scale, are commonly linked to glacial events, e.g. outburst of glacial meltwaters normal to the ice margin.</p>	

Class	Wavelength	Height	Bedform Description	Data Example
R-I	n/a	Up to 10 m	In contrast to sediment waves these features are not related to currents but present a surface expression of an underlying geological unit, e.g. chalk.	



As mentioned in section 2.2, in literature, dunes are generally understood as mobile systems that usually migrate in the direction of the residual current. Based on the orientation of identified dunes of various scales, there are two dominating current directions within the investigated area approximately flowing from (1) north to south and (2) south-east to north-west.

A comparison of the bathymetry datasets from 2012 and 2016, presented in Figure 2.5, shows a shift of class D-II dunes in the north and east, of 25 to 50 m towards the south can be measured, confirming the mobility of dunes. Furthermore, SBP data clearly shows a layer of loose sediment between the base and the crest of the dune. Due to the lack of overlapping data, the migration speed of south-east to north-west trending D-I dunes cannot be investigated at this stage.

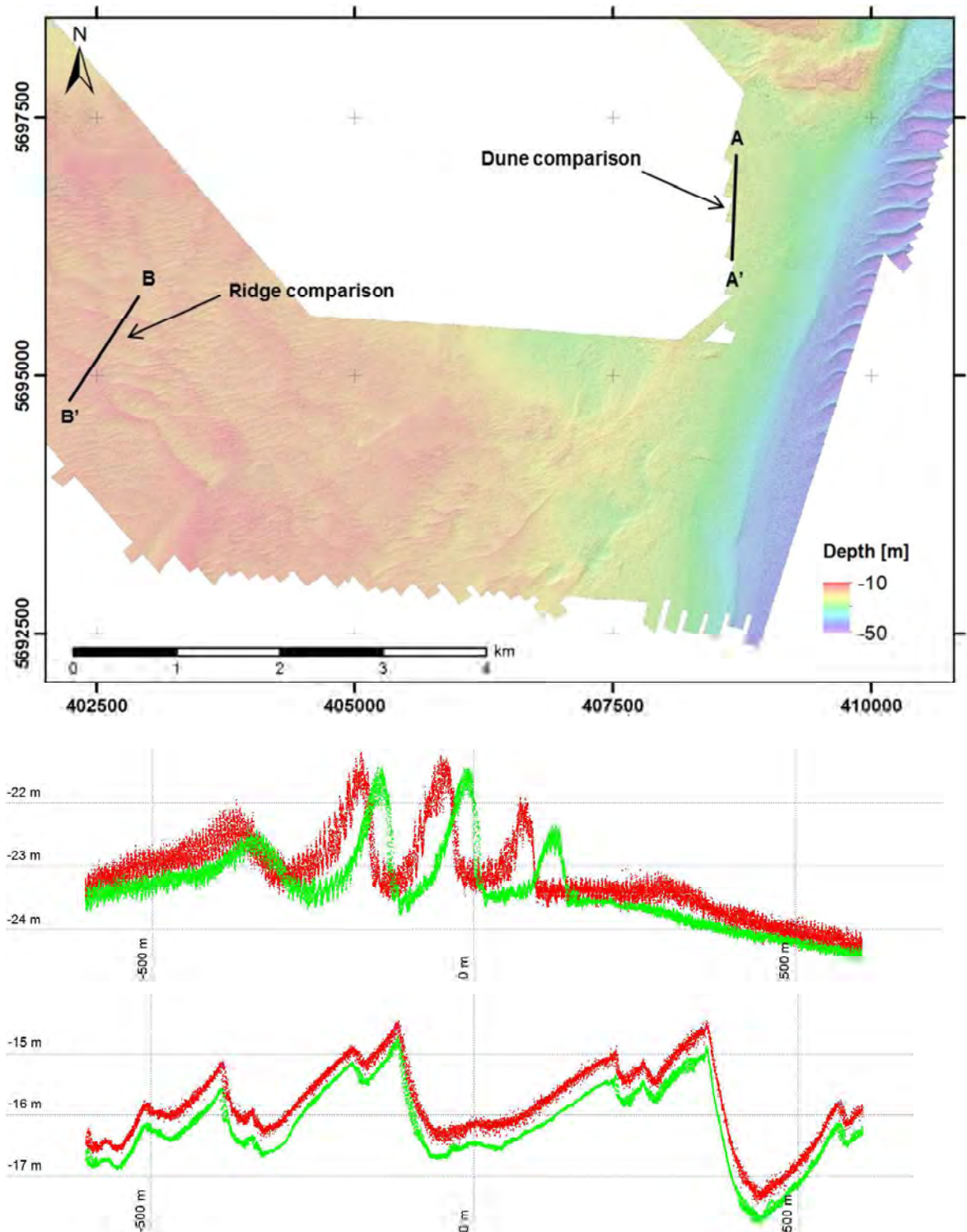


Figure 2.5: Comparison of bathymetry data from 2012 and 2016 over very large dunes and ridges (red profile: 2012 green profile: 2016)

In contrast, R-II ridges have remained stagnant over the last four years. Furthermore, sub-bottom data reveals that a layer of loose sediment between peak and base of the ridge is missing. Occasionally small amounts of sediment are deposited on the crest, however these are unrelated to the ridge formation. The dune-like shape is following the underlying chalk layer suggesting that the ridges are

part of this unit. A comparison with the MBES data acquired during the 2012 survey shows no significant changes. This can be interpreted to be the result of a starved system with little or no supply of sediments to allow the formation of dunes. The shape of the ridges is thought to be related to current-induced erosion and the dipping underlying chalk.

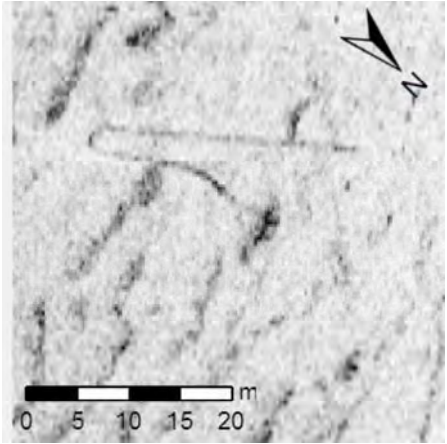
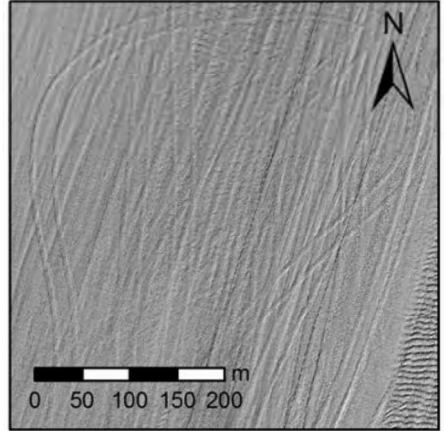
2.4 Seabed Contacts

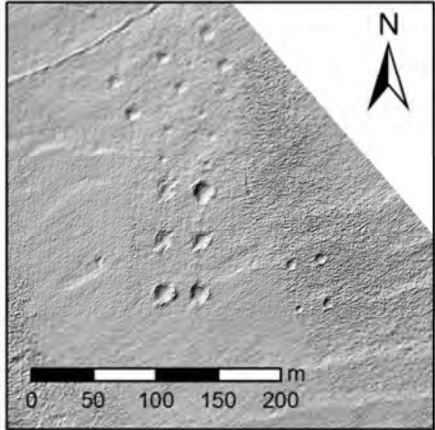
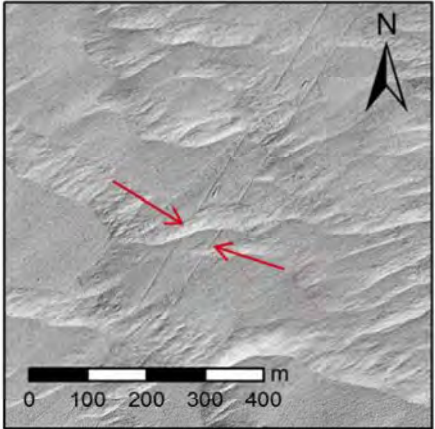
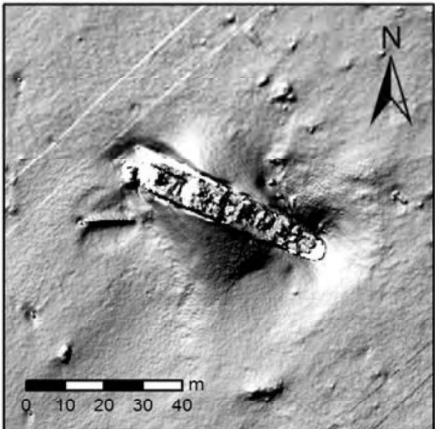
All anthropogenic seabed features described above are shown on the **Seabed Contact Charts** in Appendix D.

This section describes identified seabed features of both natural and anthropogenic origin. Most examples provided in Table 2.5 are taken from the hill-shaded bathymetry dataset as it is found to better pronounce features with small relief.

A number of man-made features are identified from SSS, MBES and MBBS data and comprise linear debris, trawling, anchor and anchor pull-out scars, spudcan depressions and cables. A complete list of all seabed targets is included in the GIS deliverables.

Table 2.5: Overview and Data Examples of Anthropogenic Seabed Contacts

Seabed Contacts	Dimension & Description	Data Example
(Linear) debris	Linear debris include but are not limited to (anchor-) chains, ropes, fishing gear, small cable or pipe sections. A total of 7 linear debris items are found in MBES and MBBS data and a further 38 debris or suspected debris items are identified from SSS data. Lengths of objects vary between approximately 1 and 270 m. The example to the right shows a possible fish trap with attached line taken from low-frequency SSS records.	
Anchor (pull-out) and trawl scars	Seabed scars from anthropogenic activity are mostly related to anchoring and fishing/trawling. Typical but not mandatory characteristics are anchor pull-out scars at one end of the scar or a set of two parallel scars indicative for trawling tracks (see example on the right). Man-made seabed scars are highly abundant in the north-north-west and south-east of the survey site and, to a lesser extent, in the central-west.	

Spudcan depressions	Spudcan depressions usually appear in sets of three (triangle), four (square) or six (rectangle) depending on the type of rig/barge that was used. Due to the occurrence of mobile sediments at this site, a complete set of depressions is not always visible. A total of 29 depressions are identified in MBES data. These are limited to a small area in the central west part of the survey site. Dimensions range between 6.9 and 17.5 m in length, 6.8 and 16.6 m in width, and 0.2 and 0.7 m in depth.	
Cables	The survey area is crossed by several cables. The presence of some of them is confirmed by MBES, SSS and, partially, SBP and MAG data. A further five uncharted cables or cable segments are identified which presumably present disused or newly laid ones. As most cables are trenched and buried, only the remaining linear elevation is visible in sonar data rather than the actual object. Further details are provided in Table 2.6.	
Shipwrecks	A total of nine shipwrecks are identified from MBES, MBBS, SSS and MAG data within the survey site. A list of their position is provided in Table 2.7.	

A total of seven (7) cables cross the TEOW based on the ENC and Admiralty charts ([Ref. 7](#)). Refer to Table 2.6 for details. Two (2) cables were not detected by any geophysical survey equipment.

Table 2.6: Cables crossing TEOW

Cable	Magneto-meter	SSS	MBES	Remarks
Thanet Export Cable (North)	YES	YES	YES	Up to 3 m offset with respect to the database position
Thanet Export Cable (South)	YES	YES	YES	Up to 5 m offset with respect to the database position

Cable	Magneto-meter	SSS	MBES	Remarks
Rembrandt 2	NO	NO	YES	Up to 33 m offset with respect to the database position
Hermes South	NO	YES	YES	Up to 5 m offset with respect to the database position
UK-Belgium 5	NO	NO	NO	Not observed
Unknown 1	NO	NO	NO	Not observed
Unknown 2	YES	NO	NO	Up to 200 m south of the database position

A total of nine (9) wrecks were observed within the TEOW. Their as-found coordinates are provided in Table 2.7.

Table 2.7: As-found wreck locations across the Thanet Extension Site

Wreck	Easting [m]	Northing [m]	Detected on:			Remarks
			Magneto-meter	SSS	MBES	
ThanetExt_FP_S0005	405318	5701990	YES	YES	YES	
ThanetExt_FP_S0080	409886	5698585	YES	YES	YES	
ThanetExt_FP_S0114	397195	5703004	YES	YES	YES	Large area of metallic debris.
ThanetExt_FP_S0151	398740	5701262	YES	YES	YES	
ThanetExt_FP_S0187	399876	5700387	YES	YES	YES	
ThanetExt_FP_S0189	399934	5701756	YES	YES	YES	
ThanetExt_FP_S0210	400726	5703005	YES	YES	YES	
ThanetExt_FP_S0878	402849	5695343	YES	YES	YES	
ThanetExt_FP_S1060	405076	5695282	YES	YES	YES	

Three additional charted wrecks were not found during this survey. Wreck locations are seldom reliable as often their final positions are last known or mayday positions instead of the actual sinking location. These positions are also often derived from less accurate positioning systems.

The magnetometer did not detect these wrecks because they might have been constructed from non-magnetic materials, but this could not be confirmed by the database description.

2.5 Other Contacts

Within the survey site 1230 SSS contacts were digitised, with heights ranging from 0.0 m (non-measurable height) up to 7.6 m (ship wreck, highest non-wreck contact is 1.6 m). These targets were categorised according to feature class and certainty. The majority of the targets (1115) were identified as boulders. The complete list of contacts can be found in the GIS deliverables and is plotted on the **Contact** chart in Appendix D.

A total of 664 magnetometer contacts were detected within the Thanet Extension Wind Farm. These magnetic anomalies range between 0.4 nT/m and 5468 nT/m. Of those contacts, 85 can be related to

sidescan sonar contacts, of which 80 were related to 9 wrecks. A total of 60 magnetometer contacts can be correlated with the existing infrastructure (cables).

The magnetic data was also assessed to see if any geological information could be extracted from the dataset.

For these analyses, only a few areas of the Thanet Extension Offshore Wind Farm were used. The south part of Block 1 is dominated by long wavelength and low magnetic anomalies. This type of magnetic signature can be related to geological features with a relatively large lateral extent, for example outcrops and dipping layers. Within Block 1, these long wavelength and low magnetic anomalies were observed in areas of outcrops, so this can be well correlated. In Block 3 no specific correlation could be made with the geology, i.e. the chalk outcrop.

Where interpretation of the contacts was possible it was correlated within the GIS Database. The locations are plotted on the **Magnetometer Ribbon Charts** in Appendix D. A contact summary is presented in Table 2.8.

Table 2.8: Summary table for SSS and magnetometer contacts

Sensor	Target classification	No. targets
SSS	Suspected debris	39
	High backscatter	6
	Wrecks	9
	Boulder	1115
	Depression	14
	Mound	2
	Fish traps	3
	Possible buried boulder/outcrop	42

Sensor	Target classification		No. targets
MAG	Unknown		524
	Cables	Thanet Export Cable North	23
		Thanet Export Cable South	20
	Wrecks		80
	Unknown cable		17

2.6 Regional Geology

The survey area is located in the southern North Sea, offshore United Kingdom. The area is situated on the London-Brabant massif that formed a structural high in Paleozoic times.

During the Triassic the southern North Sea was dominated by rifting processes, forming a sedimentary basin as a set of narrow rifts and grabens formed, causing subsidence of the Variscan topography. The rifting process can also be related to the opening of the Atlantic Ocean.

In the late Jurassic, widespread subsidence allowed a shallow marine sediment depositional environment across the southern North Sea, this process continued in the Early Cretaceous. Around the Early Cretaceous, lithospheric extension and localised rifting ceased, however, it was replaced by thermal subsidence and gentle regional crustal downwarping. Towards the end of the Early Cretaceous the area where the survey area is located is characterised by deltaic, coastal and shallow

marine clastics. During the Late Cretaceous a major eustatic sea-level rise caused a maximum sea level rise of 100 m – 200 m above the current level and flooded the whole of the European area. This caused a decrease in the supply of terrigenous material but allowed extensive deposition of pure calcareous chalk on the continental shelves. A post-rift sag phase from Late Cretaceous to Present was mainly characterised by subsidence and a quiet tectonic environment in the North Sea basin. However, during the Late Cretaceous and Tertiary a few compressional tectonic pulses occurred in the southern North Sea basin. A last significant pulse during the Mid-Miocene caused a major unconformity within the basin (Figure 2.6).

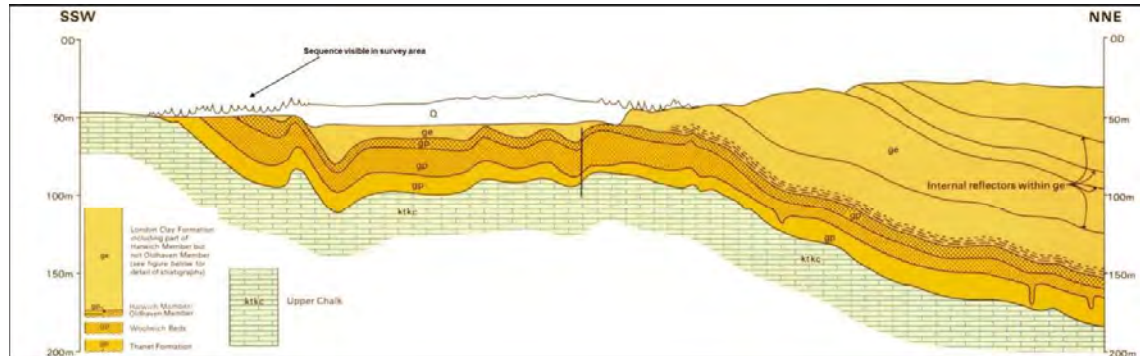


Figure 2.6: Cross section showing the Late Cretaceous to Quaternary sediments, 5 km from the survey area (modified from [ref. 8](#))

Within the Tertiary, sedimentation is dominated by marine-shelf and marginal marine depositions as a result of a succession of transgressive cycles mainly due to eustatic sea level changes. Therefore Tertiary sediments contain regional unconformities. During the Paleocene, a shallow marine environment was present in the area where the proposed wind farm location is planned, resulting in the deposition of mudstones, fine grained (decalcified glauconitic) sands or muddy sands. Neogene sediments are in general absent due to a non-depositional environment and erosional processes. However, in some areas in the North Sea basin a period of regression preceded a renewed transgression period in the latter stages of the Miocene and the earliest period in the Pliocene. During the Quaternary, deltaic systems developed in a north-west direction from continental Europe, resulting in the deposition of shallow-water and deltaic sediments. During this period, the North Sea basin has been subject to several sea level fluctuations and associated glacial and inter-glacial periods (Figure 2.7). During the interglacial periods the deposited sediments eroded and channels formed.

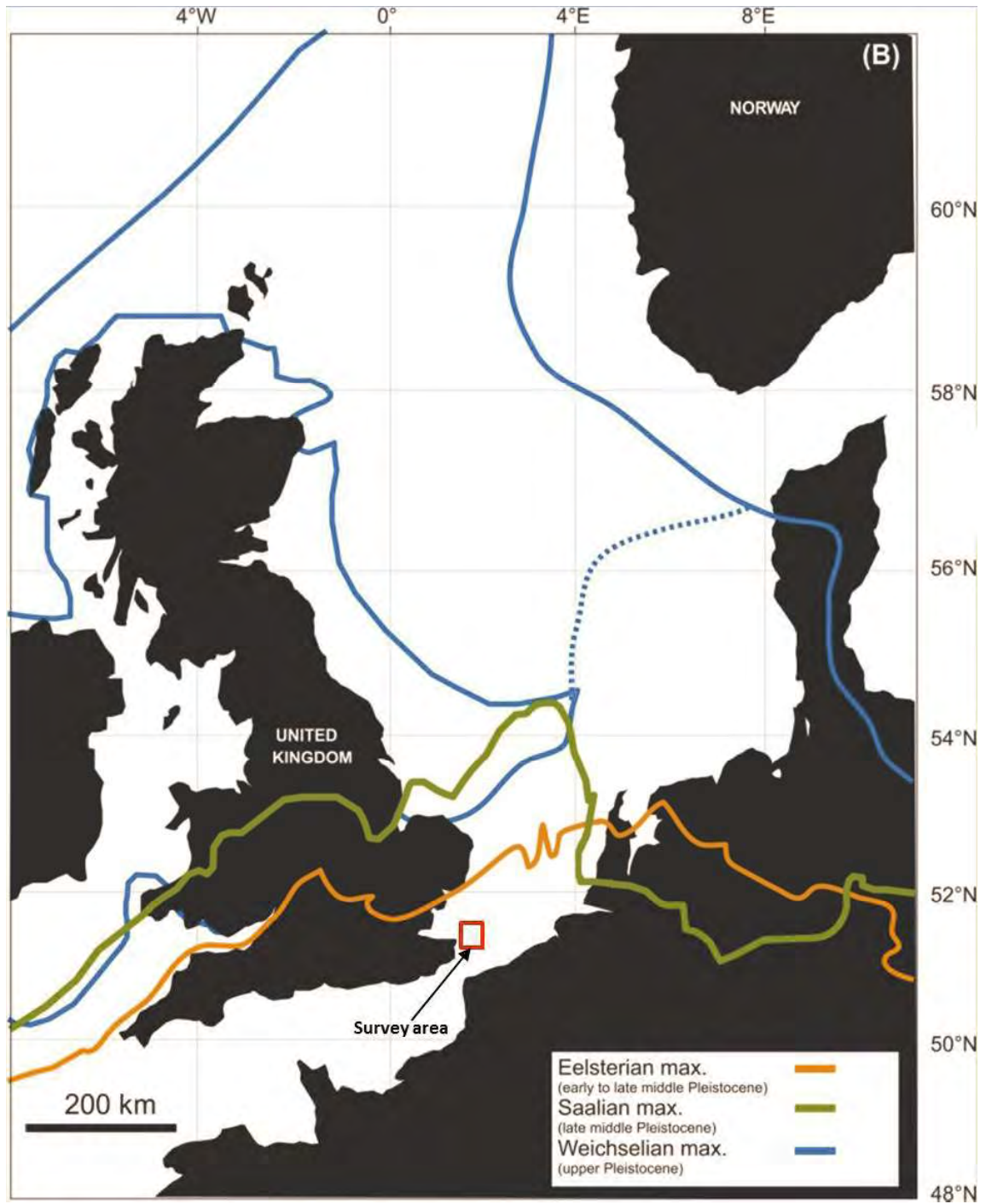


Figure 2.7: Overview of the glacial extents in the North Sea Basin during the Holocene (modified from [ref. 9](#))

2.7 Local Geology

2.7.1 Overview

The interpretation was based on multichannel sparker and air gun data. Geotechnical data were available at the time of this issue ([ref. 10](#)) and included seabed cone penetration test (CPT) and vibrocore sampling performed from the MV Bucentaur from 12 September to 16 September 2016.

This section should be read in conjunction with the **Geological Charts** in Appendix E of this report.

A seismo-stratigraphic model was derived to interpret the seismic data across TEOW. This stratigraphy is based on published geological studies ([Ref. 11](#) and [Ref. 12](#)).

The geology across the survey area down to the limit of interpretation of 250 m bsb has been subdivided in eight (8) seismic units (Units A to H). A detailed description of the interpreted seismic units is presented in Section 2.7.2. and Table 2.9.

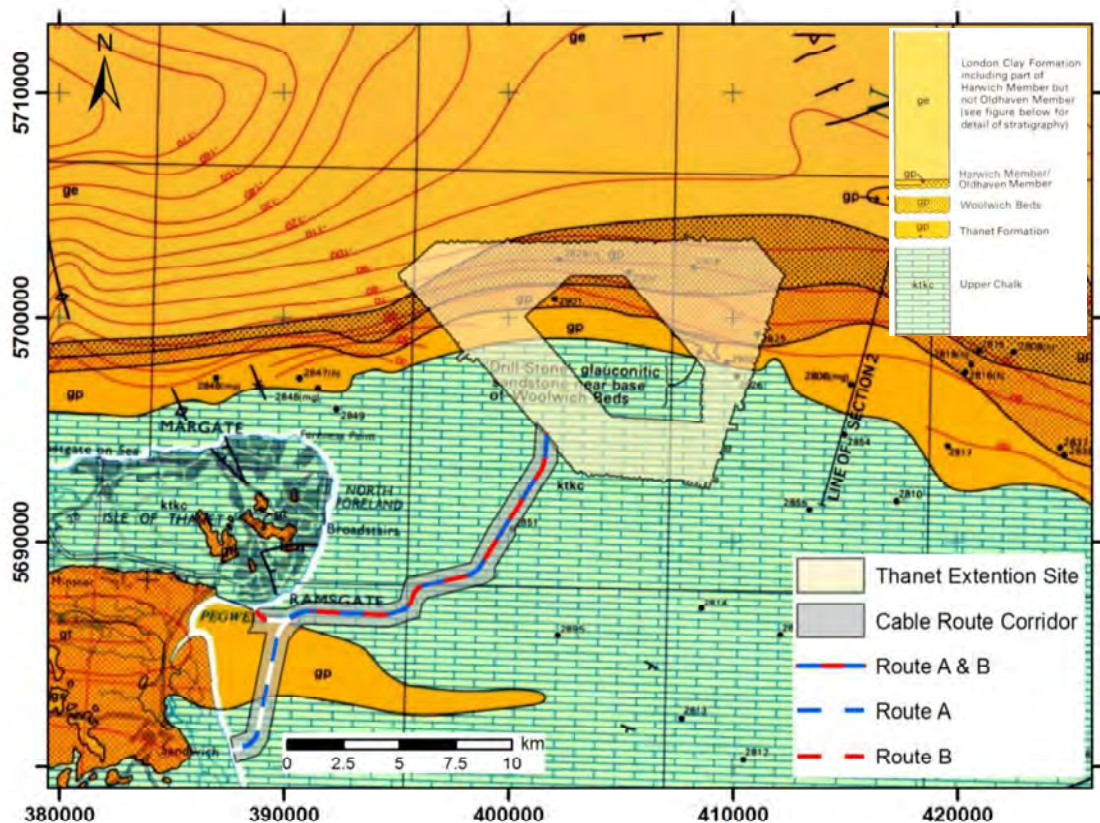


Figure 2.8: Survey area plotted on geologic chart (modified from [ref. 8](#))

Table 2.9: Overview of the interpreted seismic units

Seismic Units	Reflectors		Base of Unit min/max depth in m bLAT ⁽¹⁾	Base of Unit min/max depth in m below seabed ⁽¹⁾	Geometry of the base of the Unit	Unit seismic signature	Amplitude distribution within the Unit	Continuity of internal reflectors	Geometry of Unit	Indicative lithology ⁽²⁾	Depositional environment	Formation	Age
	Top	Base											
A	Seabed	H01	13.3 / 53.3	0 / 13.2	Erosional Surface	Sub-horizontal to cross-bedded and chaotic internal reflectors	Low to moderate	Low	Controlled at the upper boundary by sand dune morphology	Coarse SAND, with shells and shell fragments, rare SILT and CLAY laminae and rare GRAVEL	Marine	Southern Bight	Holocene
B	H01	H02	17.3 / 48.5	0 / 20.1	Erosional Surface	Parallel to sub-parallel	Medium to high	Medium to high	Channel fill	Variable sand, silt, clay and organic materials	Channel deposit	partly Elbow	Early Holocene/ Pleistocene
C	H02	H09	19 / 72	1 / 50	C1 - Undulated	Parallel to sub-parallel internal reflectors	Low to moderate	Medium to high	Sheet-like shaped	Sand overlain by marine silty clays, clayey and sandy silts, and subordinate sands	Marine	London Clay	Eocene
					C2 - Undulated	Chaotic internal reflectors	Low to high	Low	Sheet-like shaped	Glauconitic sands	Shallow-marine	Harwich?	
					C3 - Slight undulated	Chaotic internal reflectors	Moderate	Low	Sheet-like shaped		Shallow-marine	Harwich?	
					C4 - Not well defined	Not well defined	Moderate	Not well defined	Not well defined	?	?	?	?
D	H09	H10	19 / 91	1 / 74	C5 - Smooth to slight undulated	Sub-horizontal to cross-bedded internal reflectors	Low to moderate	Low to moderate	Sheet-like shaped	Complex of clays, loams and sands and pabbie beds	Shallow-marine	Woolwich	Palaeocene
					C6 - Smooth to slight undulated	Parallel to sub-parallel internal reflectors	Variable form low to high	Medium to high	Sheet-like shaped		Shallow-marine	Upnor	
					Smooth to slight undulated	Parallel to sub-parallel internal reflectors	Medium to high	Medium to high	Sheet-like shaped	Glauconitic sands, silts and silty clay with basal flint conglomerate	Shallow-marine	Thanet Formation	Palaeocene
E	H10	H20	84 / 185	67 / 164	Erosional Surface	Parallel to sub-parallel internal reflectors	Low to medium	Low to high	Sheet-like shaped	White Chalk with flint and gravels/ cobbles	Marine	Upper Chalk	Late Cretaceous
F	H20	H30	107 / 200	83 / 178	Smooth to slight undulated	Cliniform, parallel to sub-parallel internal reflectors	Variable from low to high	Low to high	Wedge shaped	Chalk with sand, silt and clay	Shallow-marine	Upper Chalk	Late Cretaceous



Seismic Units	Reflectors		Base of Unit min/max depth in m bLAT ⁽¹⁾	Base of Unit min/max depth in m below seabed ⁽¹⁾	Geometry of the base of the Unit	Unit seismic signature	Amplitude distribution within the Unit	Continuity of internal reflectors	Geometry of Unit	Indicative lithology ⁽²⁾	Depositional environment	Formation	Age
	Top	Base											
G	H30	H40	161 / 275	138 / 253	Smooth to slight undulated	Parallel to sub- parallel internal reflectors	Variable from low to high	low to high	Sheet-like shaped	Marly Chalk with flint	Marine	Middle Chalk	Late Cretaceous
H	H40	N/A	N/A	N/A	N/A	Sub-parallel internal reflectors	Variable from low to high	low to high	Sheet-like shaped	Shaly marl Chalk, hard comminuted shell-bed, calcareous clay and glauconitic marl	Marine	Lower Chalk	Late Cretaceous

Notes:
The seismic stratigraphy presented has been derived from Ref. 8

2.7.2 Local Stratigraphy

UNIT A (Seabed to Horizon H01 - Southern Bight Fm - Holocene)

The depth to the base of Unit A is presented on **Geological Chart** GE051_TE_H01 bsb_NU_20K and GE051_TE_H01 bLAT_NU_20K in Appendix E.

Unit A (Holocene in age) is observed in most of the survey area. The internal structure is characterised by discontinuous reflectors with low to medium amplitude. Very often this unit forms a veneer of sediments not resolvable by the Pinger data. The base of this Unit (Horizon H01) is predominantly an uneven sub-horizontal surface, and is interpreted to be mobile at present.

The depth to the base of Unit A ranges between 13.3 m bLAT and 53.3 m bLAT (0.0 m to 13.2 m bsb).

UNIT B (Horizon H01 – Horizon H02 – Channel deposits – Holocene/Pleistocene)

The depth to the base of Unit B is presented on **Geological Chart** GE051_TE_H02 bsb_NU_20K and GE051_TE_H02 bLAT_NU_20K in Appendix E.

Unit B is observed mostly in the northern part of the survey area. The internal structure is characterised by highly continuous medium to high amplitude reflectors. Several meandering channels were observed within this unit as isolated and amalgamated sequences (Figure 2.9).

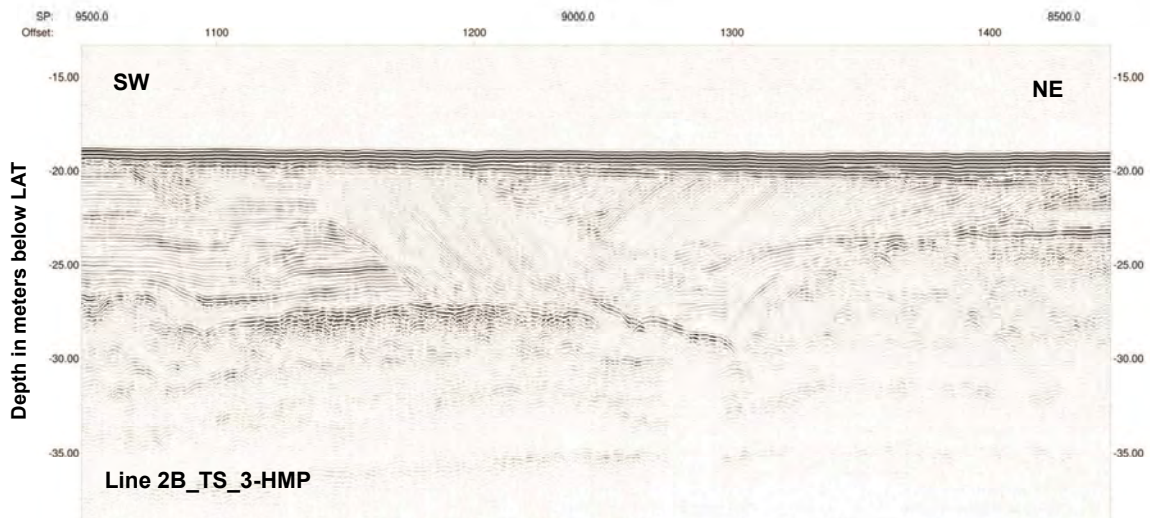


Figure 2.9: Unit B incising into underlying deposits

These deposits were interpreted as the result of the marsh and inter-tidal flat environment following the last transgression. These deposits likely contain a high percentage of organic matter accumulated inside the channels and outside in the overbank deposits and crevasse splays.

Seismic indicators (acoustic turbidity, enhanced reflectors, and diffractions) of the presence of shallow gassy sediments were observed within this unit in both SBP and UHRS data. This is likely to be the

result of the dissolving process of the organic matter content entrapped in the deeper parts of these channel infill deposits.

The depth to the base of Unit B ranges between 17.3 m bLAT and 48.5 m bLAT (0.0 m to 20.1 m bsb).

UNIT C (H02 to H09 – Thames Group to Lambeth Group – Eocene to Palaeocene)

The depth to the base of Unit C is presented on **Geological Chart** GE051_TE_H09 bsb_NU_20K and GE051_TE_H09 bLAT_NU_20K in Appendix E.

Unit C comprises a complex of vertically and laterally varying gravels, sands, silts and clays including the Thames Group and the Lambeth Group. The Lambeth Group consists of the Upnor Formation, the Woolwich Formation and the Reading Formation. The Lambeth Group is overlain by the Thames Group, which consists of two formations. From old to young these are the Harwich Formation and the London Clay Formation. This unit was divided into six sub-units, C1 through C6.

The London Clay Formation is the uppermost sub-unit of the Group. It is interpreted as sub-unit C1. This sub-unit is predominantly characterised by weak amplitude, moderate to good continuity, parallel to sub-parallel internal reflectors. The bottom of the unit is relatively higher in amplitude reflections, marked by the chaotic discontinuous reflector at the base. This unit should contain sand overlain by marine silty clays, clayey and sandy silt. Due to the erosion process during the Pleistocene age, this sub-unit only occurs within the west portion of the site.

Sub-unit C2 is generally characterised by chaotic internal reflectors with variable amplitude reflections. This sub-unit is interpreted to belong to the Harwich Formation with a thickness of up to 7 m. Based on geotechnical soil samples and the stratigraphic description in [Ref.8](#), this unit should contain glauconitic sands.

Sub-unit C3 is a thin layer with a thickness of up to 5 m. This sub-unit generally shows chaotic internal reflectors and moderate amplitude reflections. This suggests this sub-unit may predominantly contain sand. This characteristic of this sub-unit should also belong to Harwich Formation. The base of this sub-unit is delineated by weak to strong amplitude semi-continuous to good continuity reflector. Based on the stratigraphic description in [Ref. 8](#), this unit should contain glauconitic sands.

Sub-unit C4 is relatively thin, probably less than 4m. The seismic characteristic within this sub-unit is hard to define due to its thin bed. Due to the uncertainty of the seismic characteristic it is hard to define the thin stratigraphy formation.

Sub-unit C5 and C6 are interpreted to belong to the Woolwich Formation. The reflectors within these sub-units are partly masked by the presence of seabed and peg leg multiples. Due to these multiples, a strong continuous internal reflector separated between these sub-units could not be defined within the west half of the site. Sub-unit C5 is characterised by weak to moderate amplitudes, sub-horizontal to cross-bedded reflectors. The general thickness of this sub-unit is about 10 m. A few channelling systems are evident within this sub-unit. The bottom most sub-unit C6 is characterised by variable amplitudes, parallel to sub-parallel internal reflectors. The thickness of this sub-unit is generally up to



9 m. Based on the geotechnical soil samples and the stratigraphic description in [Ref. 8](#), the Woolwich formation should contain a complex of clays, loams and sands and pebble beds.

The base of the unit horizon (H09) is characterised by weak to moderate amplitude semi-continuous to good continuity reflector. This horizon is absent in the south half of the site, due to uplift and erosion events, and not distinguishable in the north-west portion due to the disruptions of seabed and peg leg multiples. The depth of the horizon ranges between 19 m and 72 m bLAT (1 m to 50 m bsb).

There are a few areas of high amplitude events present within this unit. These anomalies are interpreted to be coarser or harder sediments. Faults are evident within the north-east portion of the site.

The faults were mapped at horizon H09 in the **Geological Chart** and the channels and anomalies were mapped on the **Geohazard Chart**, in Appendix F.

VATTENFALL WIND POWER LTD.
THANET EXTENSION OFFSHORE WIND FARM GEOPHYSICAL INVESTIGATION
GEOPHYSICAL SITE SURVEY

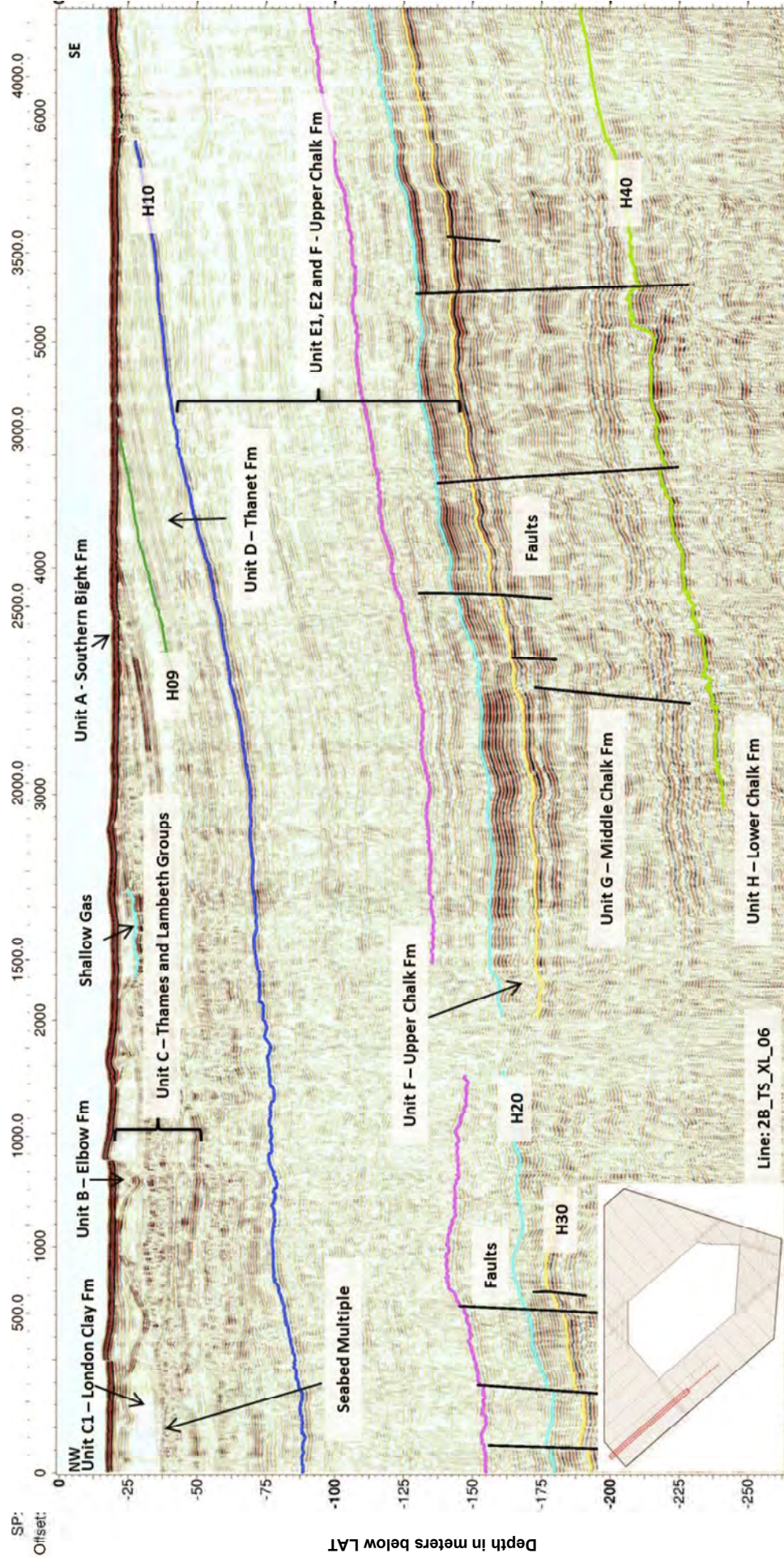


Figure 2.10: Overview of the full geologic section within the survey area

UNIT D (H09 to H10 – Thanet Formation – Palaeocene)

The depth to the base of Unit D is presented on **Geological Chart** GE051_TE_H10 bsb_NU_20K and GE051_TE_H10 bLAT_NU_20K in Appendix E.

Unit D is generally characterised by moderate to good continuity, parallel to sub-parallel internal reflectors with moderate to strong amplitude reflections. The reflectors within this unit are mostly masked by the presence of seabed and peg leg multiples. This unit was interpreted as belonging to the Thanet Formation, deposited in a shallow marine environment. Based on the stratigraphic description in Ref. 8, this unit should contain glauconitic sands, silts and silty clay with basal flint conglomerate.

The base of the unit D is Horizon 10 (H10), which is characterised by a strong amplitude good continuity reflector. This horizon is absent within the south half of the site, due to uplift and erosion events in the past. In some areas, the horizon could not be mapped out due to the disruptions of seabed and peg leg multiples. The depth of the horizon ranges between 19 m and 91 m bLAT (1 m to 74 m bsb).

Several localised minor faults are present within the unit in the west portion of the site. There are a few faults within the north-east edge and these are probably extended from the deeper units. Refer to Figure 2.11 for an overview.

The faults were mapped at horizon H10 in **Geological Chart**, in Appendix E.

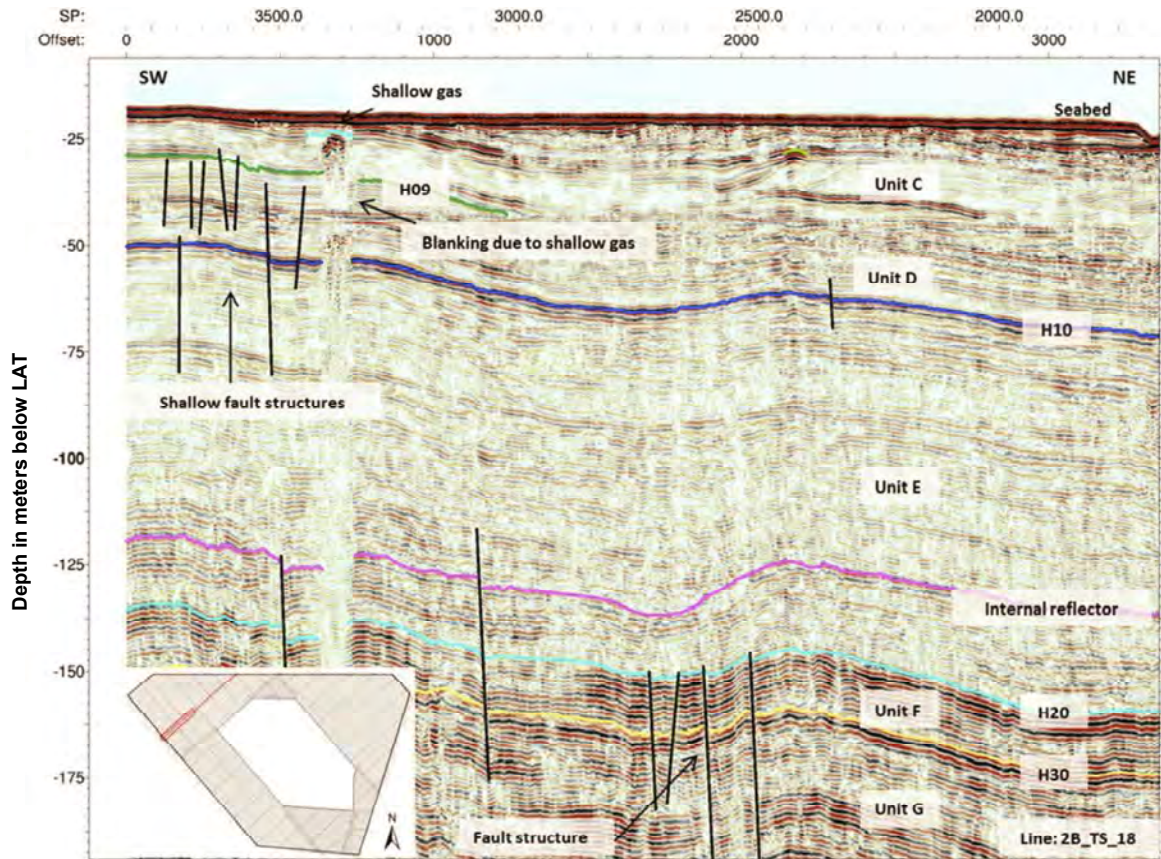


Figure 2.11: Fault structures within Unit D

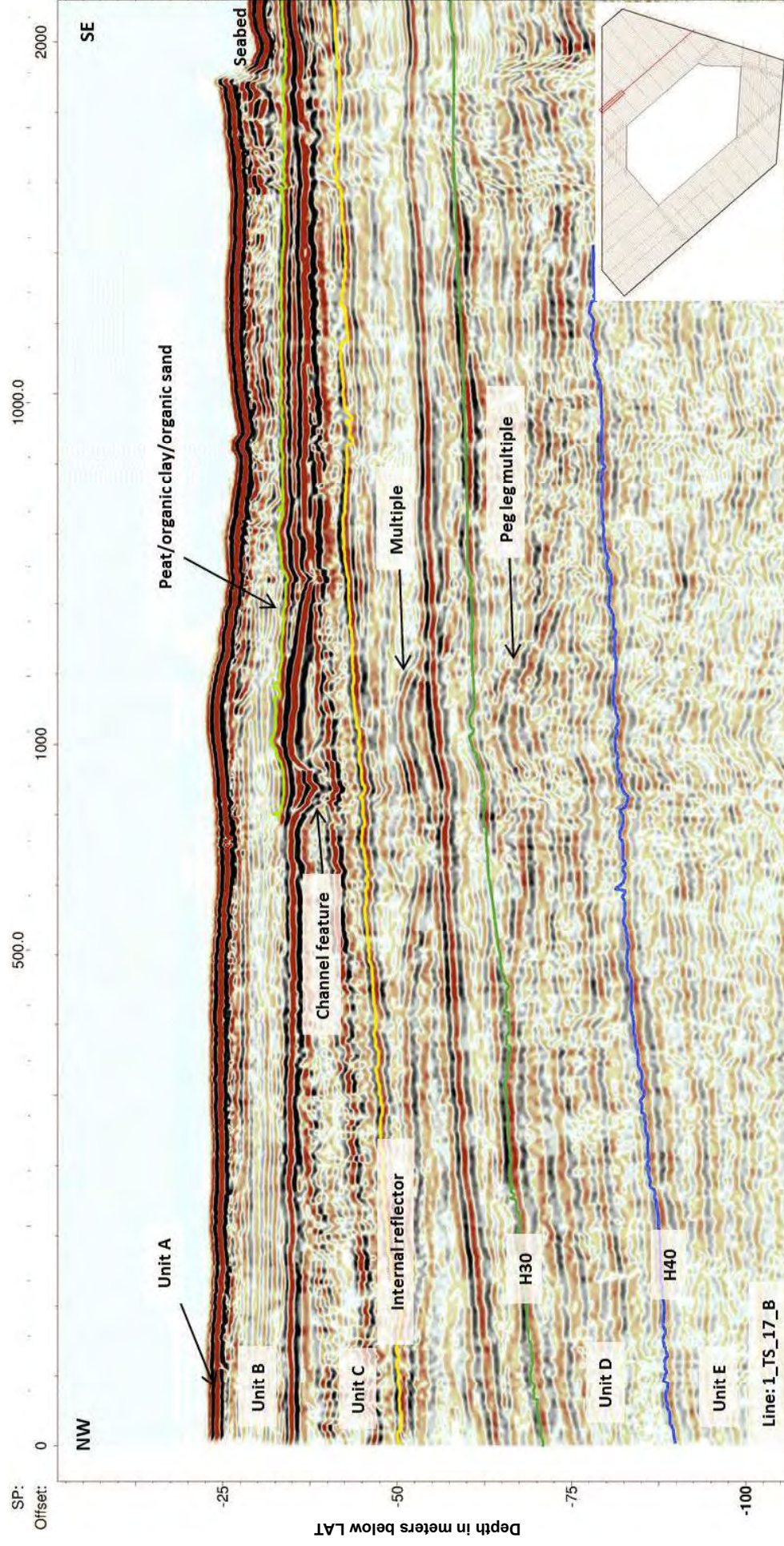


Figure 2.12: Parallel bedding within Unit D

UNIT E (H10 to H20 – Upper CHALK Formation - Upper Cretaceous)

The depth to the base of Unit E is presented on **Geological Chart** GE051_TE_H20 bsb_NU_20K and GE051_TE_H20 bLAT_NU_20K in Appendix E.

Unit E is generally characterised by poor to good continuity, parallel to sub-parallel internal reflectors with low to moderate amplitude reflections. The reflectors within this unit are partly masked by the presence of seabed and peg leg multiples. This unit was interpreted as belonging to the Upper CHALK Formation, deposited in a marine environment. Based on the acquired geotechnical soil samples and the stratigraphic description in [Ref. 8](#), this unit should contain white CHALK with flint and gravels / cobbles.

This unit was divided into two sub-units, E1 and E2, by a weak to moderately continuous reflector. This reflector is not well defined within the north-east portion and south half of the site. The depth to the base of this sub-unit (horizon H15) ranges between 84 m and 169 m bLAT (53 m to 143 m bsb).

Sub-unit E1 is generally characterised by poor to good continuity reflectors with predominantly low amplitude reflections. The top of this unit is absent and covered by veneer of Holocene sediment and possibly Quaternary infill sediments within the south half of the site due to the uplift and erosional process. The high amplitude and chaotic reflections associated with channel infills, irregular hard or coarse surface and possible shallow gas are found within this area.

In general, Sub-unit E2 shows higher amplitude reflections with a channelling system and an erosive base, possibly resulting from the last low stand period. This unit may contain CHALK with an abundance of coarser grain size sediment.

The base of Unit E is horizon H20, interpreted as an erosional surface, a weak to high amplitude, generally discontinuous to semi-continuous reflector. This reflector is faded away within the north-east portion of the site due to lack of seismic impedance changes. The depth of the horizon ranges between 107 m and 200 m bLAT (83 m to 178 m bsb).

Several localised faults are found within the upper part of sub-unit E1 extending to the overlying Tertiary formation. Some of the faults are also found to be extended from the deeper units.

Several high amplitude seismic anomalies with possible phase reversal are associated with the channels within the south portion of the site. Another acoustic turbidity area is recognised within the south-east corner of the site. These anomalies are interpreted as biogenic gas related.

Within the south-west portion, the top of CHALK is characterised by chaotic reflections with disruption below it. This irregular area is interpreted to be a harder layer or a gravelly layer.

The faults were mapped at horizon H10 in the **Geological Chart** and the channels and anomalies were mapped on the **Geohazard Chart**, in Appendix F.

VATTENFALL WIND POWER LTD.
THANET EXTENSION OFFSHORE WIND FARM GEOPHYSICAL INVESTIGATION
GEOPHYSICAL SITE SURVEY

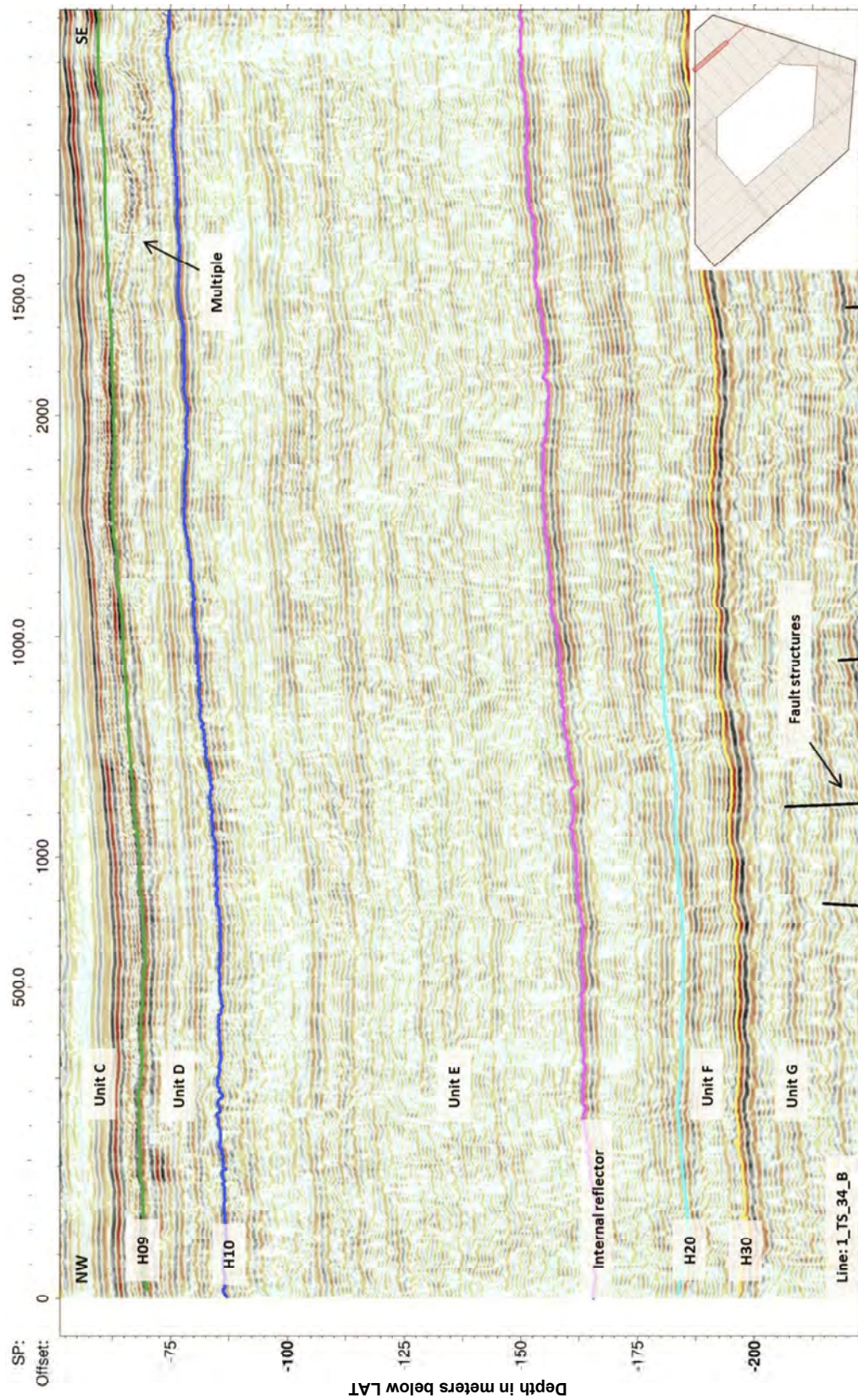


Figure 2.13: Parallel bedding within Unit E and the erosional surface H20

UNIT F (H20 to H30 – Upper CHALK Formation - Upper Cretaceous)

The depth to the base of Unit F is presented on **Geological Chart** GE051_TE_H30 bsb_NU_20K and GE051_TE_H30 bLAT_NU_20K in Appendix E.

Unit F is generally characterised by poor to good continuity, parallel to sub-parallel internal reflectors with variable amplitude reflections. The clinoform internal reflectors suggest the deposition took place during a period of sea level falling. This unit could not be correlated from the stratigraphic description in [Ref. 8](#). This CHALK unit probably consists of interlayer with clastic sediments sand, silt and clay.

The base of Unit F is horizon H30, generally high amplitude continuous reflector. This reflector is well defined throughout the site. The depth to the horizon H30 ranges between 161 m and 275 m bLAT (138 m to 253 m bsb).

Numerous faults from the deeper units are extended to this unit. These faults were mapped on the **Geological Chart**, in Appendix E.

UNIT G (H30 to H40 – Middle CHALK Formation - Upper Cretaceous)

The depth to the base of Unit G is presented on the **Geological Chart** GE051_TE_H40 bsb_NU_20K and GE051_TE_H40 bLAT_NU_20K in Appendix E.

Unit G is generally characterised by poor to good continuity, parallel to sub-parallel internal reflectors with variable amplitude reflections. This unit was interpreted as belonging to the Middle CHALK Formation, deposited in marine environment. Based on the stratigraphic description in [Ref. 8](#), this unit should contain Marly CHALK with flint.

The base of Unit G is horizon H40, a generally high amplitude continuous reflector. This reflector is not well defined within north-west portion and north-east corner of the site. The depth of the horizon ranges between 161 m and 275 m bLAT (138 m to 253 m bsb).

This unit is highly faulted due to the uplift event during the mid-Miocene. These faults were mapped on the **Geological Chart**, in Appendix E.

UNIT H (H40 to unknown– Lower CHALK Formation - Upper Cretaceous)

Unit H could only be clearly defined from the mini airgun data. This unit is characterised by poor to good continuity, sub-parallel internal reflectors with variable amplitude reflections. This unit was interpreted as belonging to the Lower CHALK Formation, deposited in marine environment. Based on the stratigraphic description in [Ref. 8](#), this unit should contain shaly marl CHALK, hard comminuted shell-bed, calcareous clay and glauconitic marl.

Faults and channels are evident within this unit; however these features could not be fully resolved due to the poor resolution data within this depth.



The base of this unit was not mapped out due to attenuation of the sparker penetration in most areas and it falls beyond the interest of the development depth.

VATTENFALL WIND POWER LTD.
THANET EXTENSION OFFSHORE WIND FARM GEOPHYSICAL INVESTIGATION
GEOPHYSICAL SITE SURVEY

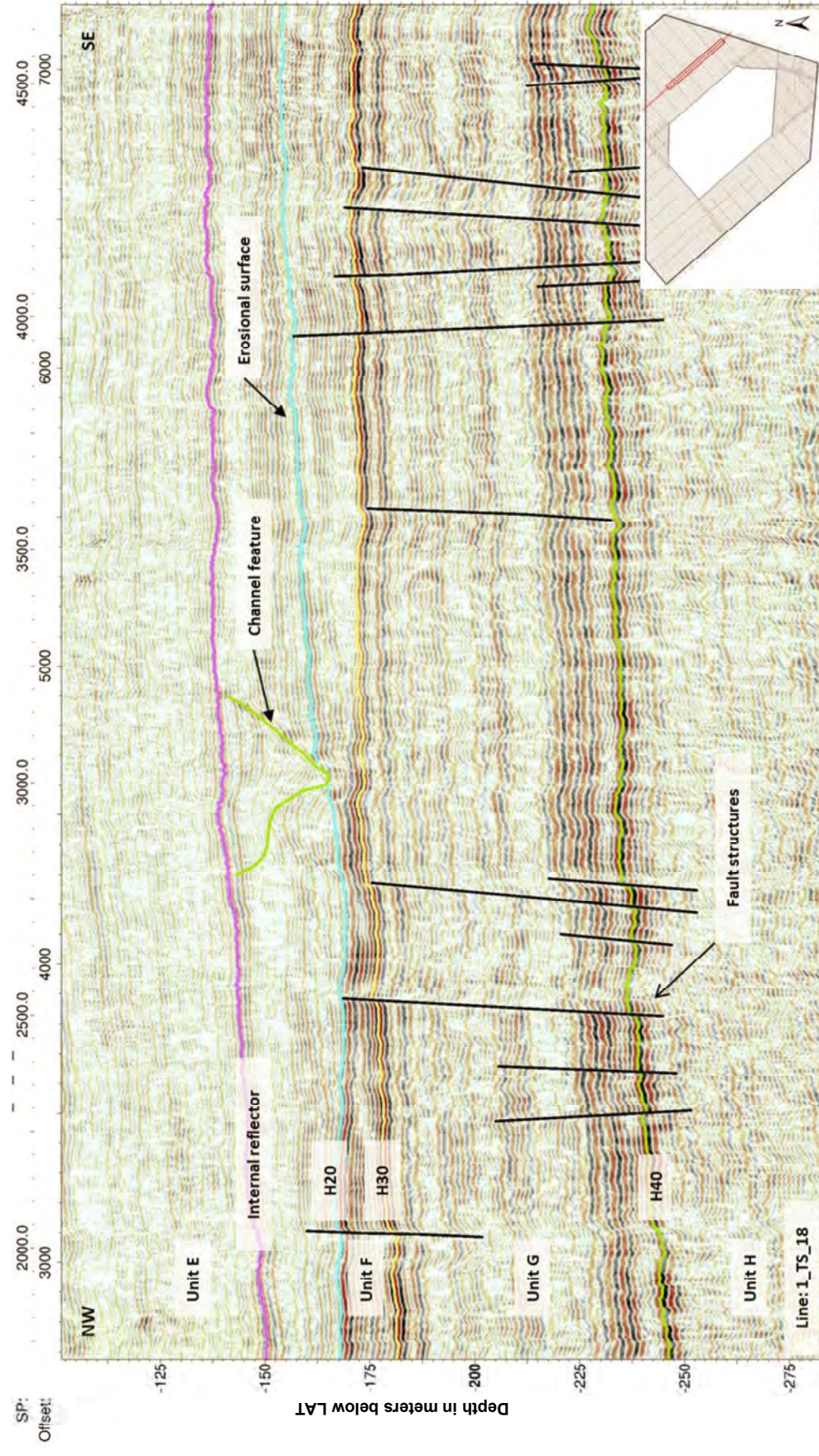


Figure 2.14: Units E, F, G and H including fault structures within Unit F, G and H and a channel structure within Unit E

2.8 Installation Constraints

This section summarizes the potential seabed hazards and subsurface geohazards to engineering work identified on the geophysical data across the Thanet Extension site. The results are also presented in the **Geohazard Charts**, Appendix F.

The following main geohazards were identified:

- **Existing infrastructure, cable, wrecks, pipeline:**
 - **Cables:** Seven (7) cables and nine (9) wrecks were observed in the TEOW.
- **Seabed hazards:**
 - **Seabed gradients:** Local seabed gradients in the north-east sector of the survey area often exceed 20 degrees and reach a maximum of about 32 degrees.
 - **Other contacts:** numerous suspected debris and unknown magnetometer contacts were observed scattered across TEOW.
- **Sub-seabed geohazards**
 - **Palaeochannel Infills (2.8.1):** Buried channels have been identified across Unit B, Unit C and Unit E with variable orientation and depths.
 - **Coarse Sediments / GRAVEL Layers / Boulders (2.8.2):** Patches of hard layers / GRAVEL layers were identified in the western and eastern portions of the site within Unit C at variable depths.
 - **Peat or Organic Sand / Clay Layers and/ or Shallow Biogenic Gas Accumulations (2.8.3):** Most of the interpreted shallow gas is associated with shallow channels. Possible peat layers or organic sand / clay are also found along the base of Unit B.
 - **Faulting (2.8.4):** Sedimentary units are moderately faulted due to the uplift events and differential compactions.

2.8.1 Palaeochannel Infill

Palaeochannel infills are heterogeneous and can pose an engineering hazard due to lateral changes in mechanical resistance. Buried channels have been identified across Unit B, Unit C and Unit E.

The base of Unit B is an erosional surface with several complex channelling systems along the unit. Due to the complexity of the channels, only the horizon contours to the base of unit B were presented on the **Geological Chart** in Appendix E.

There are several localised infill areas found within the south part of the site with a prominent long standing channel trending in south-west to north-east direction. The depths of these infills are generally shallow with the deepest depth approximately 8 m bsb. These infills are interpreted to have been developed during the Quaternary period.

A few channelling systems are evident within sub-unit C5. The channel to the west of the site is generally trending in north-west to south-east direction. Due to the seabed and peg leg multiples; this channel could not be fully mapped.

Another deep channel, trending in north to south direction, was found in Unit E. This channel is not well defined in some areas. The approximate edges of these channels have been plotted on the **Geohazards Chart** in Appendix F.

2.8.2 Coarser Sediments / GRAVEL Layers / Boulders

Reflectors with positive high amplitudes in UHR and strong chaotic diffractions in pinger data interpreted as patches of hard layers/GRAVEL layers were identified in the west and east portions of the site within Unit C (see Figure 2.15).

Additionally individual parabolic diffractions based on pinger data were mapped as the probable presence of boulders. These features are generally scattered within the south-west half of the site.

These features were mapped on the **Geohazard Charts** in Appendix F.

2.8.3 Peat or Organic Sand / Clay Layers and/ or Shallow Biogenic Gas Accumulations

The UHR and the pinger data were both analysed for seismic indicators of shallow biogenic gas charged sediments and / or peat and the results were compared. However, the data quality below the first and second seabed multiples is lower and small anomalies may not have been identified due to the system limitations.

There are several areas of shallow gas indications within the site, mostly associated with shallow channels. These areas show high amplitude, reverse polarity, locally a frequency attenuation of the reflector underneath, velocity pull-down and acoustic blanking of the deeper layers.

A large patch of acoustic turbidity, low to high amplitude with disruption underneath is found within the south-east portion. Another small patch with similar seismic attributes is found to the north-east. These anomalies are interpreted to have a high probability of being gas related.

Few small patches of high amplitude reverse polarity reflectors were found within Unit C in the west portion of the site. No attributes are found to suggest that these anomalies are gas related but rather lithology related.

A large area of moderate amplitude with reverse polarity reflector was mapped along the base of Unit B within the north portion of the site. This anomaly is interpreted to represent peat or organic sand / clay layers.

These anomalies were mapped on the **Geohazard Charts** in Appendix F.

VATTENFALL WIND POWER LTD.
THANET EXTENSION OFFSHORE WIND FARM GEOPHYSICAL INVESTIGATION
GEOPHYSICAL SITE SURVEY

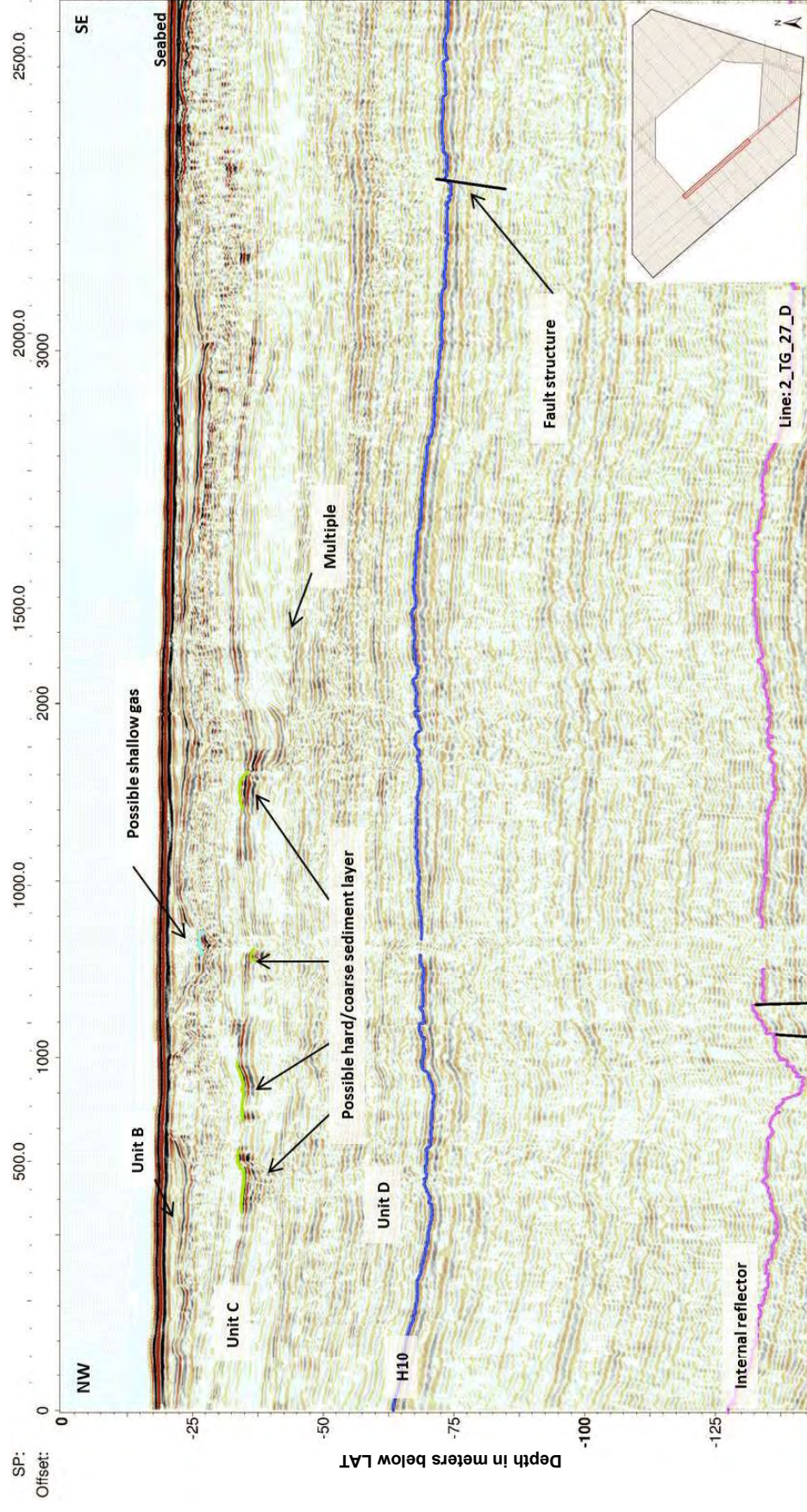


Figure 2.15: Possible hard/coarse sediment layer



2.8.4 Faulting

Normal faults are evident from the pinger and UHR data. The sedimentary units are moderately faulted due to the uplift events during the mid-Miocene period. The strike and the dipping of the faults vary across the site. Some of the faults are found extended to the base of Unit B within the north-east portion of the site. Due to the short lateral extent of some of the faults, it was not possible to always laterally trace them. Trends were only mapped if the same fault was observed in at least two survey lines.

There are numerous small differential compaction faults along the base of Unit C and they can only be clearly seen at the west portion of the site. The lateral thickness change of overlying facies, are the basic controlling factors of these differential compaction faults. These faults are generally displaced about 1 m, with possible striking along the slope.

The lateral, shallowest and deepest extent of the faults could not be fully resolved due to the limitation of vertical data resolution.

Refer to Figure 2.11 and Figure 2.14 for data examples of the faults within the site.

These faults were only mapped at each horizon on the **Geological Chart** in Appendix E.

3. DATA REDUCTION AND PROCESSING

3.1 Positioning and Navigation

All raw DGPS data were edited to remove erroneous fixes. No smoothing filters were applied to the position data during acquisition.

The antenna position was corrected to the vessel common reference point position (CRP) using measured offsets, during the acquisition of data. The position of the antenna during the analogue programme was corrected for layback of each towed instrument by applying the offset along the vessel track.

Real-time logging of navigation was acquired using Fugro's Starfix.Seis navigation system. Bathymetric sounding (water depth) data was logged in Kongsberg SIS software.

The processing of the acquired navigation data was carried out using the Starfix.Proc software.

The data were processed using offsets from the vessel datum for all sensors. Equipment offsets from the CRP position are presented in the **Operation and Calibrations** report (Report 1).

3.2 Multibeam Echo Sounder

3.2.1 Bathymetry Processing Workflow

Bathymetry data collected from the hull mounted dual head Kongsberg EM2040 multibeam echo sounder onboard the M.V. Fugro Pioneer was processed in Caris Hydrographic Information Processing System and Sonar Information Processing System (HIPS & SIPS). The Caris HIPS & SIPS general workflow is presented in Table 3.1.

Table 3.1: Caris HIPS & SIPS bathymetry workflow

CARIS HIPS Work Step	Description
1. Raw MBES data	MBES raw data as logged by SIS, in combination with data input from Starfix NG
2. HIPS vessel file	<p>Before data can be converted into Caris HIPS a so called HIPS Vessel File (HVF) has to be defined. This HVF contains all relevant sensor definitions with information regarding offsets, correction values and system configurations.</p> <p>The HVF defines amongst others: Offsets relative to the center of gravity (COG), Sound velocity information, Dynamic vessel motion (heading, roll, heave , pitch), Static corrections for gyro heading and error for roll, heave and yaw heading alignment of the multibeam system, Static TPU settings including offsets and survey equipment standard deviations (based on technical specifications).</p>
3. Data conversion to HIPS	The multibeam raw data exported from the online software is to be converted into HIPS format. Positioning information included in the raw data is based on geographical co-ordinates.

CARIS HIPS Work Step	Description
4. Quality control (Navigation, Attitude data)	Navigation & attitude data were checked for spikes. This is done manually or by using self-defined filters. Spikes are marked and flagged as not to be used for further calculation. The resulting gaps are interpolated over time by calculating new values.
5. Swath filter	Depth information of one survey line is filtered for spurious values and data not to be used. Filter settings for flagging data as rejected can include the following settings: Min-max. accepted depth range, Across track angle of beam to beam slopes, Angle from nadir, The filters are applied according to the encountered morphology, weather condition etc. The applied values may vary from area to area. Nevertheless, each line is checked separately and the filter parameters are adapted if necessary.
6. Tide reduction	All water depths will be referenced to LAT, reduced using post processed GPS height data collected in real time on board the vessel. GNSS heights were referenced to LAT by using the Vertical Offshore Reference Frame (VORF) model. Processing GNSS heights is done within Fugro Starfix.VBAProc and applied to the bathymetry in Caris HIPS & SIPS.
7. Sound velocity correction	Each survey line is corrected for sound velocity. The sound velocity table contains date, depth and correction values for each profile and is applied to each survey line. It can be chosen, whether a profile shall be supplied previous or nearest in time or nearest in distance.
8. Calculation of final position and depth for each beam (data merging)	For each individual beam a position and a depth value is calculated with respect to vessel (gyro) heading, tide data (including dynamic draft) and sound velocity correction using time as correlation.
9. Create work surfaces	The pre-checked data is used to calculate a CUBE surface.
10. Surface filter using CUBE	The CUBE algorithm creates a hypothesis for the depth value of a grid cell from the first depth value that falls into a cell. Every following depth value is checked against this hypothesis and according to a variety of settings selected to contribute to the existing hypothesis, to create a new, second hypothesis or to be rejected. A most probable surface is resulting from these calculations. This surface is then used as a base for a surface filter, for which a data window of acceptance around this surface had to be specified using certain parameters. The survey data is then checked against these conditions. Data outside the specified window of acceptance is rejected.
11. Create quality control surfaces	New base surfaces are calculated to check the result. Having undergone these procedures, the data is in a final state for delivery. Contour calculation was achieved by using Fugro Starfix Workbench.
12. Quality control	The data quality is mainly checked using the standard deviation, density (hit count) and visual bathymetry inspection. Local anomalies are removed manually or by a local applied filter.
13. Data export	As a deliverable from HIPS a gridded data set is produced and exported as ASCII files. Additional requests such as adding line names as a fourth column and managing data size were done with Fugro Starfix.VBAProc and TextPipe

3.2.2 Bathymetry assembling

The survey line plan for data acquisition of the Thanet Extension survey area consisted of several blocks as presented in Figure 3.1. As a consequence, bathymetry data processing in Caris HIPS & SIPS was done per block as an individual project.

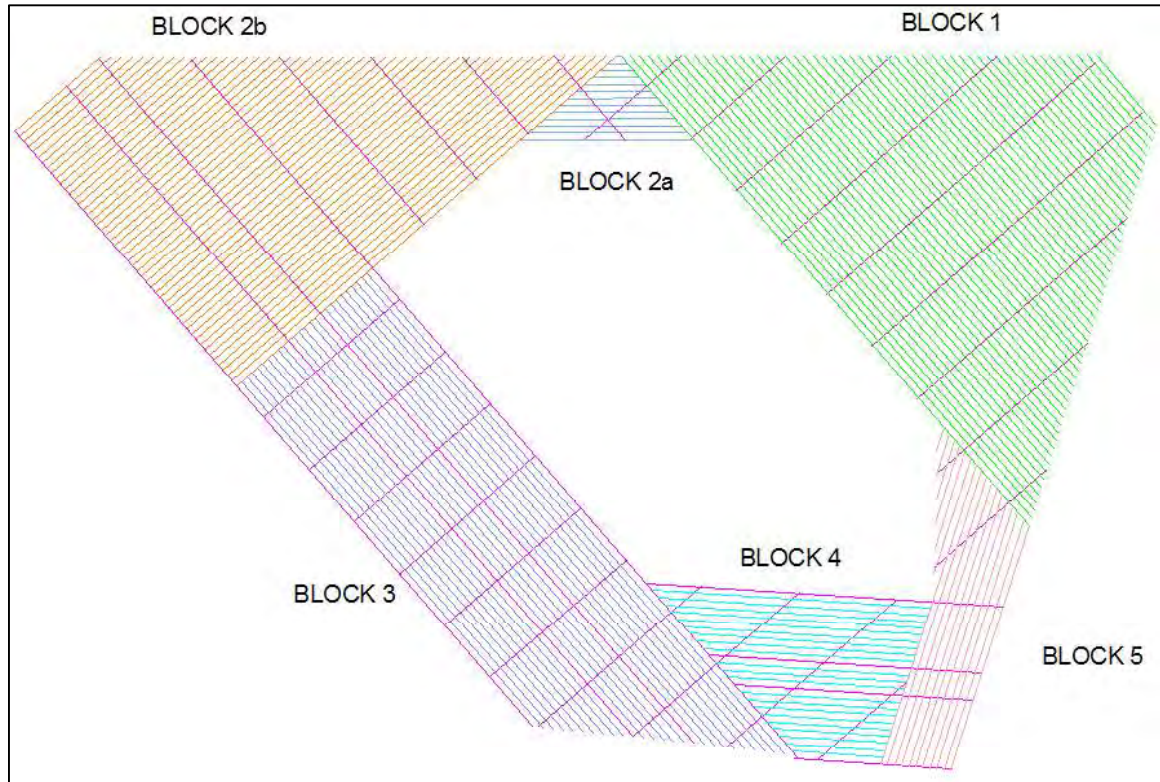


Figure 3.1: Thanet Extension block definition

Individual bathymetry blocks were combined together after processing was finalized into a single DTM covering the whole Thanet Extension survey area. The amount of data overlapping from one block into another block was reduced during this process for cosmetic purpose, primarily for the following reasons:

- i. Significant sediment movement due to date difference between acquisition of survey blocks.
- ii. Small vertical mismatches of several centimetres between individual blocks.

Additional information about each item is explained in more detail in the next sections.

Exported ungridded data is free of any clipping for cosmetic purposes as described above.

3.2.3 Sediment movements

Significant sediments movements were observed in the overlap areas between block 5 with block 1 and 4 and between block 1 and block 2a as indicated in Figure 3.2. Seabed in these indicated areas is dominated by small sand dunes.

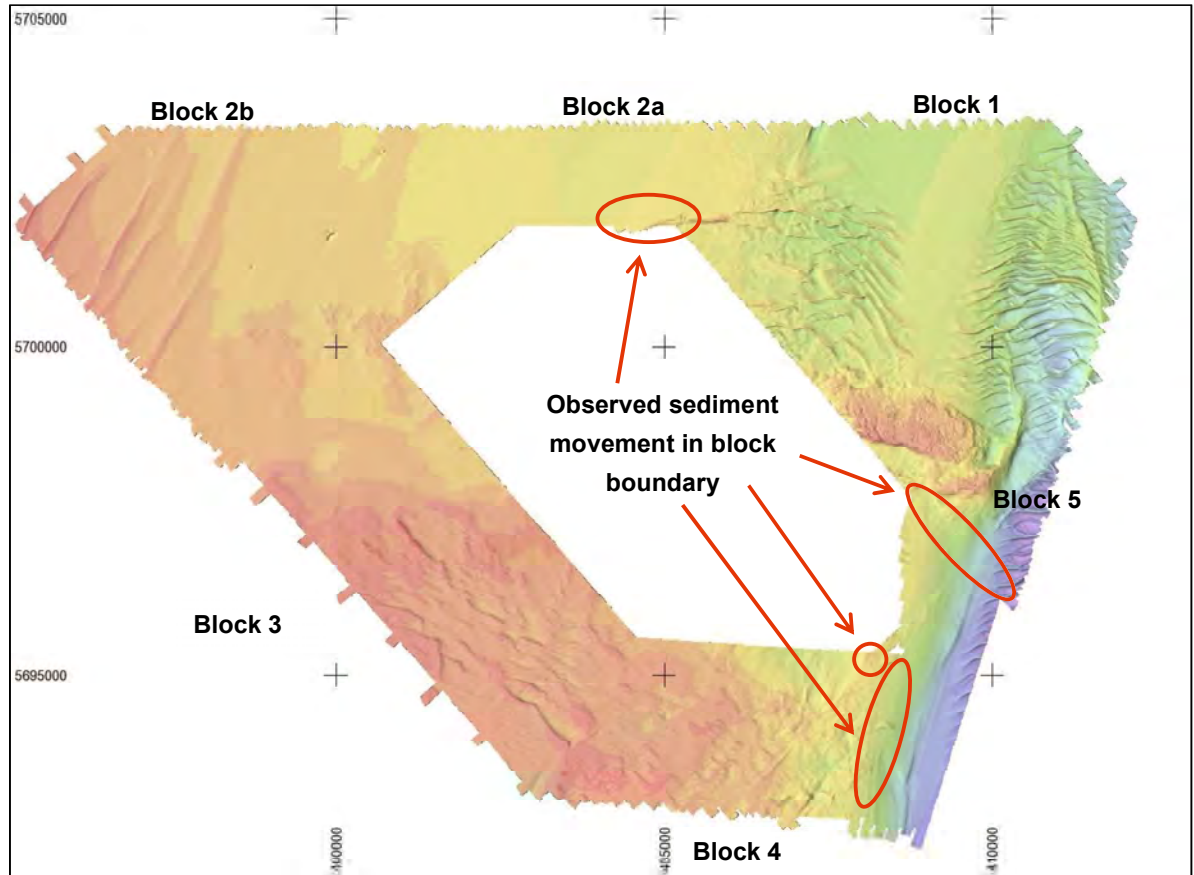


Figure 3.2: Observed sediment movement in survey block overlapping areas

Sand ripple migration was revealed in the block overlap areas where different datasets overlap which were acquired on different dates. Examples, such as presented in Figure 3.3 show a significant movement of the sand dunes between 11 August 2016 (orange) and 31 August 2016 (green). Some shifts presented in Figure 3.3 are around 3.4 m. Data gridding operations suffer from these kind of seabed difference resulting in a false flat seabed (as the crests moved to the positions of the troughs) or a shifted seabed.

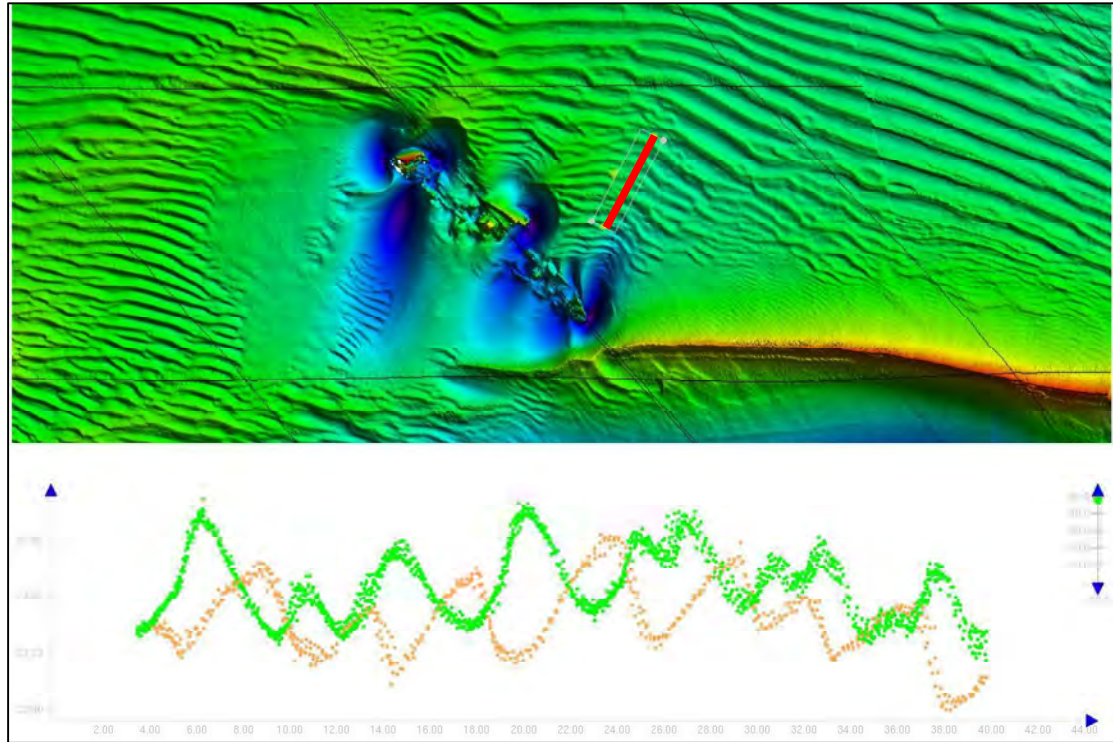


Figure 3.3: Ripple migrations between block 1 and block 2a

3.2.4 Small vertical mismatches

Small vertical mismatches (less than 5 cm) were observed between blocks 1, 2a, 2b, 3 and 4. The vertical difference between block 5 and its neighbour blocks 1 and 4 was slightly larger with an average of less than 10 cm. This slightly larger mismatch in block 5 is partly driven by significant sediment movements in the overlapping areas with block 1 and to some extent block 4.

3.3 Backscatter Data

Backscatter data collected by the MBES onboard the M.V. Fugro Pioneer was processed by using QPS Fledermaus Geocoder. Backscatter processing was divided in the same blocks as the bathymetry processing.

A correction of -1.5 dB has been applied to Block 2a and Block 2b to compensate for the decibel offset introduced by enabling the Dual Swath functionality of the Kongsberg EM2040.

Locally, small dB offsets have been applied to individual session to improve the mosaic quality. Small dB offsets (less 1 dB) were observed in all blocks (e.g. Figure 3.4).

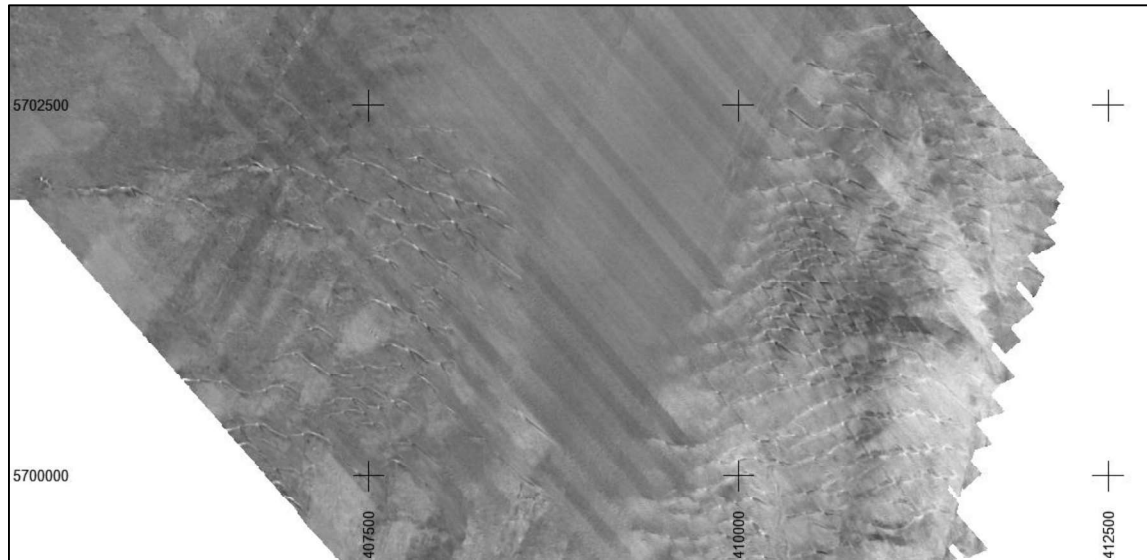


Figure 3.4: Small dB offsets in Backscatter on Block 1

Local backscatter anomalies associated to the nadir beams of the MBES could not fully be resolved during backscatter processing. Backscatter anomalies stand out clearly on the sand ripple crest in Figure 3.5. These anomalies were amplified by the use of Dual Swath which significantly increases the amount of energy in the water column. Secondly, small changes in the online acquisition setup of the MBES (such as gain, power etc.) have a influence on the backscatter quality.

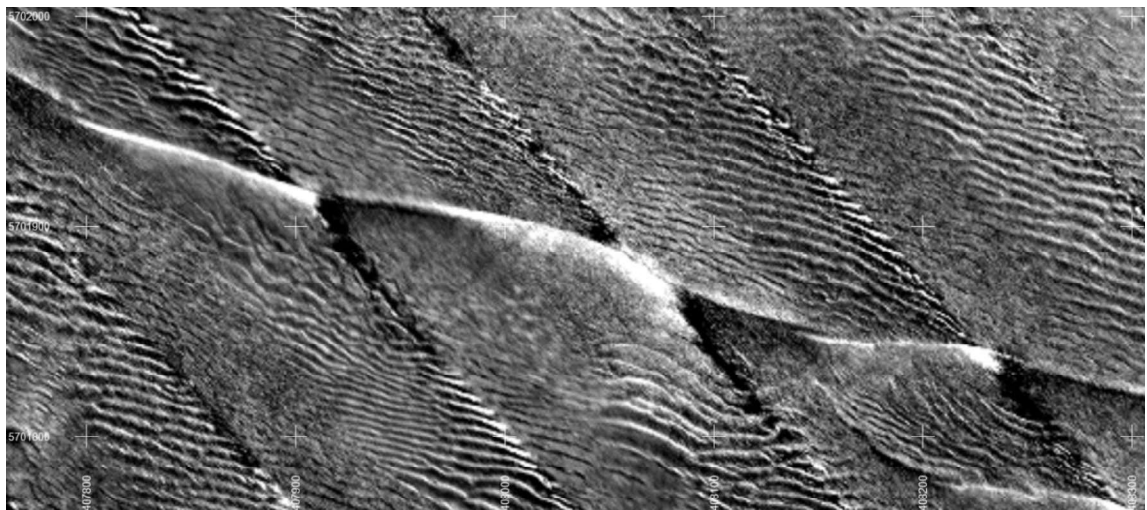


Figure 3.5: Backscatter anomaly in nadir region on sand ripple crest

3.4 Sidescan Sonar

Data were recorded in digital format (.xtf) using the Starfix GLog/GPlot software.

The records were corrected for slant-range distortion before interpretation.

The *.xtf files were imported into SonarWiz software, where a full quality control of each line was carried out. At the same time, data were analysed and checked for discrete sonar contacts, and the positions were compared with MBES data.

The SSS mosaic (GeoTiff file) was created within SonarWiz using high and low frequency data with a cell size of 0.5 m x 0.5 m.

Each SSS contact was checked for positioning against MBES data.

3.5 Magnetometer

The magnetometer data were recorded in digital format (*.pos) using the Starfix software. The navigation and altitude were manually checked and de-spiked when necessary. Quality control and processing of the magnetic data was performed in Geosoft Oasis Montaj.

The magnetometer data was subject to sparker noise generated from the acoustic signal as the sparker was towed in close proximity of the magnetometer. A series of non-linear filters were used to filter the noise and keep the initial magnetic signal. Then a B-spline filter was used to remove any high frequency, low amplitude noise. The residual magnetic signal was calculated using a combination of non-linear filters and a final B-Spline filter. Refer to Table 3.2 for an overview of the settings and sequence of the used filters. Magnetic targets, or anomalies, were identified using the Blakely Test which is a grid peak picking algorithm. Targets were picked where peaks had a grid value of > 5 nT/m and all of the nearest grid cells were lower. A QC check was performed after this picking and additional anomalies were picked when necessary.

As the sparker has not been used on all survey lines, not all magnetometer data was affected by sparker noise. Therefore the data has been split in multiple databases to obtain the best results for the magnetometer data. The range of the filters used is presented in Table 3.2.

Table 3.2: Settings and sequence of magnetometer data filters

Filter	Setting 1	Setting 2
Non Linear 1 sparker	Filter width 2	Filter tolerance 5
Non Linear 2 sparker	Filter width 1	Filter tolerance 2.5
Non Linear 3 sparker	Filter width 1	Filter tolerance 0.5
B-Spline	Smoothness 0.6	Tension 0.0
Non Linear 1	Filter width 40-50	Filter tolerance 2
Non Linear 2	Filter width 20-25	Filter tolerance 1
Non Linear 3	Filter width 10-12	Filter tolerance 0.5
Non Linear 4	Filter width 5-6	Filter tolerance 0.25
Non Linear 5	Filter width 3	Filter tolerance 0.125
B-Spline	Smoothness 0.6	Tension 0.0

A separate processing flow was used for the geological assessment that was performed on the magnetic data. As the data was not collected for this purpose, it is of lower quality than would be preferred for this type of assessment. The aim of processing the data further was to have a look at the medium and long wavelengths in the dataset, instead of only the high frequency, short wavelength content, which mainly reflects man-made objects. Medium wavelength magnetic anomalies are often

caused by geological structures like faults, volcanic dykes and channel fills. Longer wavelengths are more likely to originate from features with a greater lateral extent, e.g. outcrops and dipping layers.

Data preparation consisted of three steps. The first one was to filter out any noise that was generated by the sparker, this was done using a short non-linear filter. After this, any artefacts that were caused by on line adjustments in the SSS cable length (due to the magnetometer being piggybacked behind the magnetometer) were removed. Where necessary, lines were split and reassembled manually. Finally, a narrow low pass filter was applied before levelling the selected lines and cross-lines.

A low pass filter, followed by a sequence of very wide non-linear filters, was used to extract the long wavelengths from the dataset. The long wavelength dataset was then subtracted from the low passed dataset in order to obtain the medium wavelength dataset.

Table 3.3: Settings and sequence of magnetometer data filters for geological assessment

Filter	Setting 1	Setting 2
Non Linear 1 sparker	Filter width 1	Filter tolerance 5
Low pass	150	-
Levelling	-	-
Low pass	500	-
Non Linear 1	Filter width 1000	Filter tolerance 2
Non Linear 2	Filter width 500	Filter tolerance 1
Non Linear 3	Filter width 250	Filter tolerance 0.5
Non Linear 4	Filter width 125	Filter tolerance 0.25
Non Linear 5	Filter width 62	Filter tolerance 0.125

3.6 Sub-bottom Profiler

The quality of the sub-bottom profiler data was good.

The SBP data files were recorded using the Starfix GLog/GPlot software. Two types of data file were recorded, .glog files (as raw data) and .segy files. Heave corrections were recorded in the raw pinger data during acquisition.

Quality control consisted of checking the data for positioning errors and cross-checking with MBES and SSS data. Data were reduced to LAT using a dedicated RadExPro routine.

Several tests were carried out in order to achieve optimal results on SBP data. The optimal processing parameters were as follows;

- Low cut filter: 2000 Hz;
- High cut filter: 7500 Hz;
- Manual TVG Curve.

3.7 Data Interpretation

3.7.1 Bathymetry Data Interpretation

Bedform zonation was performed in ArcGIS (v10.3.1) software and the DTM file (cell size 0.25 m x 0.25 m) was used as basis for the interpretation. A bedform zonation map was derived from a manual demarcation of homogeneous areas in terms of sand dune shape, wavelength and crest line orientation.

The bedform zonation was exported in GeoTiff, .dwg format and .shp file.

3.7.2 Sidescan Sonar Data Interpretation

SSS records were examined both for significant targets and for the general level of backscatter from the seabed. The contacts detection on the SSS data files was done using the SonarWiz software with the SSS waterfall visualisation for optimal resolution. Targets with dimensions above 1.0 m were picked. Smaller target sizes were also picked where the resolution of the data was sufficient. Where objects were detected their geographic location was logged, together with their length, width, height and identification.

The level of confidence achieved for target picking is generally good for the high frequency SSS data. Due to adverse sea state conditions in combination with shallow water depths, noise was observed towards the limit of the SSS range on the high frequency data. The confidence level of the target picking was good up to a range of 40 to 60 m. Beyond this range, a lower confidence level was achieved. However, considering the significant overlap and coverage achieved, and the additional use of the low frequency SSS data, the confidence level for the central 10 m corridor between the main survey lines is moderate. Each SSS contact was checked for positioning against MBES data.

3.7.3 Magnetometer Data Interpretation

All the magnetic targets were picked using Oasis Montaj (v8.5).

Magnetometer targets were automatically picked on the analytic signal gridded data using a threshold of 5 nT/m for the magnetic anomalies. The picked targets were individually reviewed to assess the veracity of the Oasis Montaj algorithm. During this review, artefacts were manually deleted from the target database.

Besides individual magnetic objects, the majority of the cables and pipelines from the database present in the survey area were identified by the magnetometer data.

All as-found magnetic anomalies were cross-referenced with the SSS and MBES data.

3.7.4 Seismic Data Interpretation and Gridding Methodology

The interpretation of the processed geophysical data was performed using Kingdom software (v 8.8). The UHR seismic lines imported into Kingdom were converted to metres using a smoothed velocity field, while the SBP seismic lines were interpreted in time and then the surfaces converted to metres, using a constant velocity of 1600 m/s for the shallow sediment. True amplitude SEGYS were chosen

for the interpretation instead of equalized ones in order to better understand the relative amplitudes of the main horizon and to investigate the possible presence of shallow gas and/or peat layers.

The interpretation of the seismic data is based on the recognition of sedimentary facies, layer continuity and the seismic texture of layers identified in the seismic profiles. Eight (8) seismic units were identified across the survey area. Subsequently these units were incorporated into the geological framework derived from previous desk studies and geological references in the area. The final geological model of the area is based on the depth converted UHR post-stack time-migrated profiles.

After interpretation the following features were mapped:

- Depth to base on the significant reflections;
- Locations of any structural complexities or geo-hazards within the shallow geological succession such as faulting, accumulations of shallow gas or buried channels.

The line spacing for SBP and UHR data was 100 m for the main lines and 1000 m for the cross lines, features smaller than these distances may not have been detected.

For each interpreted horizon two different surfaces were created, one in metres below LAT and one in metres below the seabed. The depth below seabed was calculated by subtracting the depth of the seabed picked on the UHR data from the depth of the picked horizon. A grid surface was then created from these values.

The gridding was performed from each interpreted horizon with the exception of H01 using Kingdom software v 8.8. The cell size was chosen taking into account the seismic profiles resolution, the line spacing and the geological surfaces spatial variability. The gridding algorithm used was *minimum curvature*, and then contours were created for each surface, parameters are presented in Table 3.4. In particular, this algorithm could be modified with the following parameters:

- Search distance (to look for data): enter the maximum projection distance from a control point to a point inside the grid. Grid values will not be generated further than this distance from the nearest input value location. Where there are large gaps in the interior of data sets being gridded, this parameter is useful for suppressing the output of grid values of dubious usefulness. Similarly, for 2D data sets having highly irregular exterior boundaries, this parameter can control the projection of the grid into areas of no control.
- Smoothness: could be adjusted from minimum (1) to maximum (11) values in order to apply less or more smoothing.

Table 3.4: Gridding and contouring methodology and parameters

Grids	Gridding parameters					Contours parameters	
	Gridding method	Source data	Cell size (m)	Smooth	Search Distance	Threshold (m)	Sampling increment
H02 bLAT/bsb	Minimum curvature	SBP, UHR	25 x 25	6	10	30	2
H09 bLAT/bsb	Minimum curvature	SBP, UHR	25 x 25	11	10	30	2
H010 bLAT/bsb	Minimum curvature	UHR	25 x 25	11	10	30	2
H020 bLAT/bsb	Minimum curvature	UHR	25 x 25	11	10	30	2
H030 bLAT/bsb	Minimum curvature	UHR	25 x 25	11	10	30	2
H040 bLAT/bsb	Minimum curvature	UHR	25 x 25	11	10	30	2

The results of the interpretation are as follows:

- Contour maps (isolines) of the significant geological formations as depth to top of formation below (bsb);
- Contour maps (isolines) of the significant geological formations as depth to top of formation below (LAT).

The results were drawn in AutoCAD 2015.

4. REFERENCES

Reference 1: Ashley et al. (1990). Classification of large-scale subaqueous bedforms: A new look at an old problem. *Journal of Sedimentary Petrology*, vol. 60, No. 1, January, 1990, pp. 160-172

Reference 2: Németh et al. (2002). Modelling sand wave migration in shallow shelf seas. *Continental Shelf Research*, vol. 22, pp. 2795 - 2806

Reference 3: Tonnon et al. (2006). The morphodynamic modelling of tidal sand waves on the shoreface. *Coastal Engineering*, vol. 54, pp. 279 – 296

Reference 4: Stow et al. (2009). Bedform-velocity matrix: The estimation of bottom current velocity from bedform observations. *Geology*, vol. 37, pp. 327 – 330

Reference 5: Pearce et al (2014). Repeated mapping of reefs constructed by *Sabellaria spinulosa* Leuckart 1849 at an offshore wind farm site. *Continental Shelf Research*, vol. 83, pp. 3 - 13

Reference 6: Presentation by Muffy Seiderer (2013): Balancing the provision of infrastructure enhancements against their environmental cost

Reference 7: <http://mapgateway.findmaps.co.uk/wms/>

Reference 8: Thames Estuary (Sheet 51N – 00) – British Geological Survey. 1:250 000

Reference 9: Alastair G.C. Graham, Martyn S. Stoker, Lidia Lonergan, Tom Bradwell, Margaret A. Stewart (2010) The Pleistocene Glaciations of the North Sea basin.

Reference 10: Geotechnical Report Field Operations and Results report. Thanet Extension Offshore Windfarm Geotechnical Site investigation 2016. Fugro Document No.: GE051/WPE-01(02)

Reference 11: Thanet Offshore Wind LTD. Post Construction Geophysical Surveys – Spring 2012. Gardline Project Ref. 9078. 2012

Reference 12: Thanet Offshore Wind LTD – Geophysical Survey – Final Report. Ref 4306r1. 2005



APPENDICES

- A. TRACK CHARTS
- B. BATHYMETRY CHART
- C. SEABED AND SEDIMENT CLASSIFICATION CHARTS
- D. CONTACT CHARTS
- E. GEOLOGICAL CHARTS
- F. GEOHAZARD CHART
- G. UHR SEISMIC PROCESSING REPORT



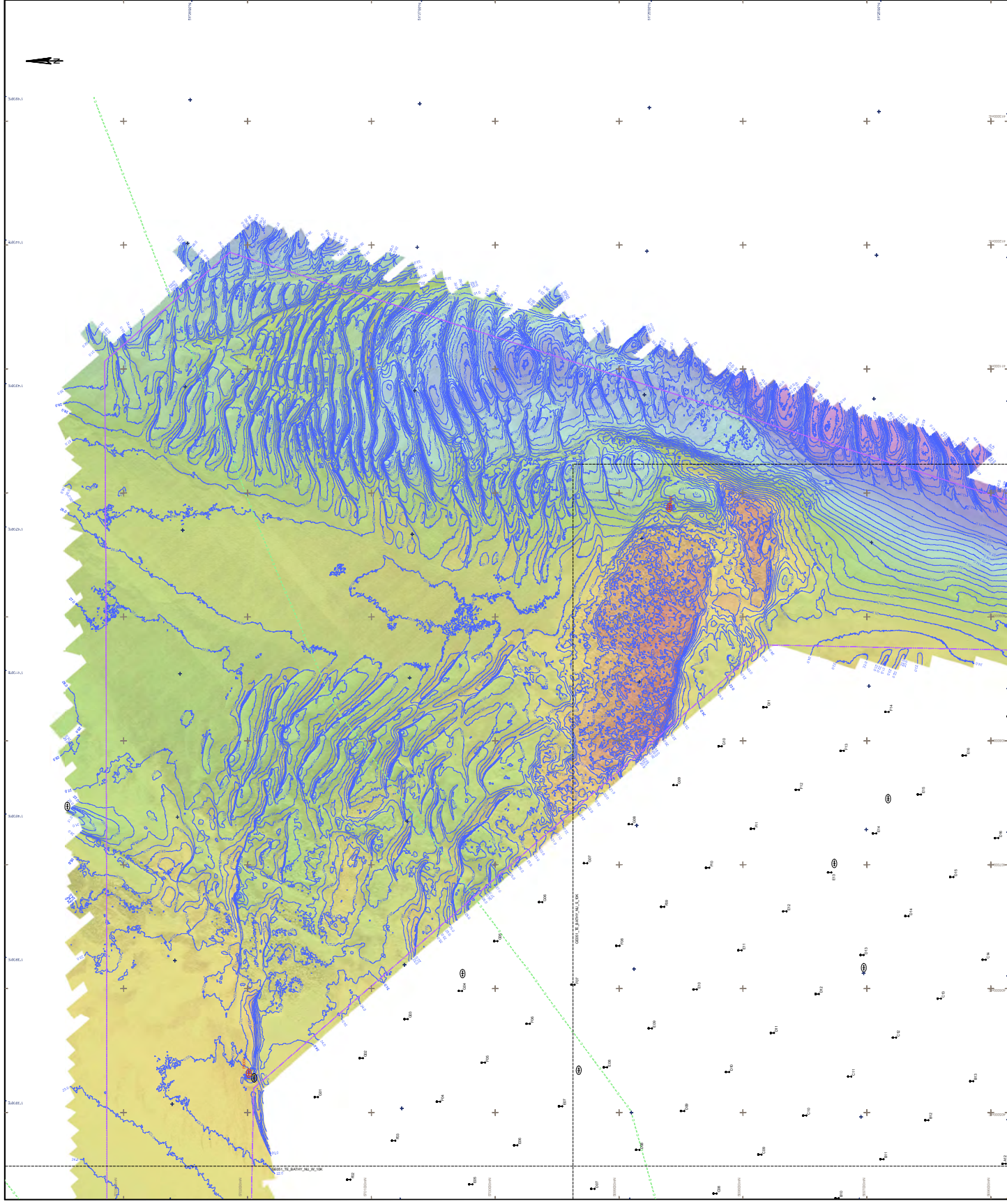
A. TRACK CHARTS

Drawing	Chart Name	Scale
Track Plot Magnetometer	GE051_TE_TRACK-MAG_NU_10K	1 : 10,000
Track Plot Multibeam	GE051_TE_TRACK-MBE_NU_10K	1 : 10,000
Track Plot Sub-bottom Profiler	GE051_TE_TRACK-SBP_NU_10K	1 : 10,000
Track Plot Sidescan Sonar	GE051_TE_TRACK-SSS_NU_10K	1 : 10,000
Track Plot UHR Sparker	GE051_TE_TRACK-UHR_NU_10K	1 : 10,000



B. BATHYMETRY CHART

Drawing	Chart Name	Scale
Shaded Relief Bathymetry Chart	GE051_TE_BATHY_NU_10K	1 : 10,000



LEGEND:

GENERAL

- UTM GRID
- GEODINAMICAL GRID
- DEEP FINE GRID (0.5M)
- WIND FARM BOUNDARY (100M)
- WIND FARM BOUNDARY (500M)
- WIND FARM BOUNDARY (1000M)
- WIND FARM BOUNDARY (2000M)
- WIND FARM BOUNDARY (4000M)
- WIND FARM BOUNDARY (8000M)
- WIND FARM BOUNDARY (16000M)
- WIND FARM BOUNDARY (32000M)
- WIND FARM BOUNDARY (64000M)
- WIND FARM BOUNDARY (128000M)
- WIND FARM BOUNDARY (256000M)
- WIND FARM BOUNDARY (512000M)
- WIND FARM BOUNDARY (1024000M)
- WIND FARM BOUNDARY (2048000M)
- WIND FARM BOUNDARY (4096000M)
- WIND FARM BOUNDARY (8192000M)
- WIND FARM BOUNDARY (16384000M)
- WIND FARM BOUNDARY (32768000M)
- WIND FARM BOUNDARY (65536000M)
- WIND FARM BOUNDARY (131072000M)
- WIND FARM BOUNDARY (262144000M)
- WIND FARM BOUNDARY (524288000M)
- WIND FARM BOUNDARY (1048576000M)
- WIND FARM BOUNDARY (2097152000M)
- WIND FARM BOUNDARY (4194304000M)
- WIND FARM BOUNDARY (8388608000M)
- WIND FARM BOUNDARY (16777216000M)
- WIND FARM BOUNDARY (33554432000M)
- WIND FARM BOUNDARY (67108864000M)
- WIND FARM BOUNDARY (134217728000M)
- WIND FARM BOUNDARY (268435456000M)
- WIND FARM BOUNDARY (536870912000M)
- WIND FARM BOUNDARY (1073741824000M)
- WIND FARM BOUNDARY (2147483648000M)
- WIND FARM BOUNDARY (4294967296000M)
- WIND FARM BOUNDARY (8589934592000M)
- WIND FARM BOUNDARY (17179869184000M)
- WIND FARM BOUNDARY (34359738368000M)
- WIND FARM BOUNDARY (68719476736000M)
- WIND FARM BOUNDARY (137438953472000M)
- WIND FARM BOUNDARY (274877906944000M)
- WIND FARM BOUNDARY (549755813888000M)
- WIND FARM BOUNDARY (1099511627776000M)
- WIND FARM BOUNDARY (2199023255552000M)
- WIND FARM BOUNDARY (4398046511104000M)
- WIND FARM BOUNDARY (8796093022208000M)
- WIND FARM BOUNDARY (17592186044416000M)
- WIND FARM BOUNDARY (35184372088832000M)
- WIND FARM BOUNDARY (70368744177664000M)
- WIND FARM BOUNDARY (140737488355328000M)
- WIND FARM BOUNDARY (281474976710656000M)
- WIND FARM BOUNDARY (562949953421312000M)
- WIND FARM BOUNDARY (1125899906842624000M)
- WIND FARM BOUNDARY (2251799813685248000M)
- WIND FARM BOUNDARY (4503599627370496000M)
- WIND FARM BOUNDARY (9007199254740992000M)
- WIND FARM BOUNDARY (18014398509481984000M)
- WIND FARM BOUNDARY (36028797018963968000M)
- WIND FARM BOUNDARY (72057594037927936000M)
- WIND FARM BOUNDARY (144115188075855872000M)
- WIND FARM BOUNDARY (288230376151711744000M)
- WIND FARM BOUNDARY (576460752303423488000M)
- WIND FARM BOUNDARY (1152921504606846976000M)
- WIND FARM BOUNDARY (2305843009213693952000M)
- WIND FARM BOUNDARY (4611686018427387904000M)
- WIND FARM BOUNDARY (9223372036854775808000M)
- WIND FARM BOUNDARY (18446744073709551616000M)
- WIND FARM BOUNDARY (36893488147419103232000M)
- WIND FARM BOUNDARY (73786976294838206464000M)
- WIND FARM BOUNDARY (147573952589676412928000M)
- WIND FARM BOUNDARY (295147905179352825856000M)
- WIND FARM BOUNDARY (590295810358705651712000M)
- WIND FARM BOUNDARY (1180591620717411303424000M)
- WIND FARM BOUNDARY (2361183241434822606848000M)
- WIND FARM BOUNDARY (4722366482869645213696000M)
- WIND FARM BOUNDARY (9444732965739290427392000M)
- WIND FARM BOUNDARY (18889465931478580854784000M)
- WIND FARM BOUNDARY (37778931862957161709568000M)
- WIND FARM BOUNDARY (75557863725914323419136000M)
- WIND FARM BOUNDARY (151115727451828646838272000M)
- WIND FARM BOUNDARY (302231454903657293676544000M)
- WIND FARM BOUNDARY (604462909807314587353088000M)
- WIND FARM BOUNDARY (1208925819614629174706176000M)
- WIND FARM BOUNDARY (2417851639229258349412352000M)
- WIND FARM BOUNDARY (4835703278458516698824704000M)
- WIND FARM BOUNDARY (9671406556917033397649408000M)
- WIND FARM BOUNDARY (19342813113834066795298816000M)
- WIND FARM BOUNDARY (38685626227668133590597632000M)
- WIND FARM BOUNDARY (77371252455336267181195264000M)
- WIND FARM BOUNDARY (154742504910672534362390528000M)
- WIND FARM BOUNDARY (309485009821345068724781056000M)
- WIND FARM BOUNDARY (618970019642690137449562112000M)
- WIND FARM BOUNDARY (1237940039285380274899124224000M)
- WIND FARM BOUNDARY (2475880078570760549798248448000M)
- WIND FARM BOUNDARY (4951760157141521099596496896000M)
- WIND FARM BOUNDARY (9903520314283042199192993792000M)
- WIND FARM BOUNDARY (19807040628566084398385987584000M)
- WIND FARM BOUNDARY (39614081257132168796771975168000M)
- WIND FARM BOUNDARY (79228162514264337593543950336000M)
- WIND FARM BOUNDARY (158456325028528675187087900672000M)
- WIND FARM BOUNDARY (316912650057057350374175801344000M)
- WIND FARM BOUNDARY (633825300114114700748351602688000M)
- WIND FARM BOUNDARY (1267650600228229401496703205376000M)
- WIND FARM BOUNDARY (2535301200456458802993406410752000M)
- WIND FARM BOUNDARY (5070602400912917605986812821504000M)
- WIND FARM BOUNDARY (10141204801825835211973625643008000M)
- WIND FARM BOUNDARY (20282409603651670423947251286016000M)
- WIND FARM BOUNDARY (40564819207303340847894502572032000M)
- WIND FARM BOUNDARY (81129638414606681695789005144064000M)
- WIND FARM BOUNDARY (162259276829213363391578010288128000M)
- WIND FARM BOUNDARY (324518553658426726783156020576256000M)
- WIND FARM BOUNDARY (649037107316853453566312041152512000M)
- WIND FARM BOUNDARY (1298074214633706907132624082305024000M)
- WIND FARM BOUNDARY (2596148429267413814265248164610048000M)
- WIND FARM BOUNDARY (5192296858534827628530496329220096000M)
- WIND FARM BOUNDARY (10384593717069655257060992658440192000M)
- WIND FARM BOUNDARY (20769187434139310514121985316880384000M)
- WIND FARM BOUNDARY (41538374868278621028243970633760768000M)
- WIND FARM BOUNDARY (83076749736557242056487941267521536000M)
- WIND FARM BOUNDARY (166153499473114484112975882535043072000M)
- WIND FARM BOUNDARY (332306998946228968225951765070086144000M)
- WIND FARM BOUNDARY (664613997892457936451903530140172288000M)
- WIND FARM BOUNDARY (1329227995784915872903807060280344576000M)
- WIND FARM BOUNDARY (2658455991569831745807614120560689152000M)
- WIND FARM BOUNDARY (5316911983139663491615228241121378304000M)
- WIND FARM BOUNDARY (10633823966279326983230456482242756608000M)
- WIND FARM BOUNDARY (21267647932558653966460912964485513216000M)
- WIND FARM BOUNDARY (42535295865117307932921825928971026432000M)
- WIND FARM BOUNDARY (85070591730234615865843651857942052864000M)
- WIND FARM BOUNDARY (170141183460469231731687303715884105728000M)
- WIND FARM BOUNDARY (340282366920938463463374607431768211456000M)
- WIND FARM BOUNDARY (680564733841876926926749214863536422912000M)
- WIND FARM BOUNDARY (1361129467683753853853498429727072845824000M)
- WIND FARM BOUNDARY (2722258935367507707706996859454145691648000M)
- WIND FARM BOUNDARY (5444517870735015415413993718908291383296000M)
- WIND FARM BOUNDARY (10889035741470030830827987437816582766592000M)
- WIND FARM BOUNDARY (21778071482940061661655974875633165533184000M)
- WIND FARM BOUNDARY (43556142965880123323311949751266331066368000M)
- WIND FARM BOUNDARY (87112285931760246646623899502532662132736000M)
- WIND FARM BOUNDARY (174224571863520493293247799005065324265472000M)
- WIND FARM BOUNDARY (348449143727040986586495598010130648530944000M)
- WIND FARM BOUNDARY (696898287454081973172991196020261297061888000M)
- WIND FARM BOUNDARY (1393796574908163946345982392040522594123776000M)
- WIND FARM BOUNDARY (2787593149816327892691964784081045188247552000M)
- WIND FARM BOUNDARY (5575186299632655785383929568162090376495104000M)
- WIND FARM BOUNDARY (11150372599265311570767859136324180752990208000M)
- WIND FARM BOUNDARY (22300745198530623141535718272648361505980416000M)
- WIND FARM BOUNDARY (44601490397061246283071436545296723011960832000M)
- WIND FARM BOUNDARY (89202980794122492566142873090593446023921664000M)
- WIND FARM BOUNDARY (178405961588244985132285746181186892047843328000M)
- WIND FARM BOUNDARY (356811923176489970264571492362373784095686656000M)
- WIND FARM BOUNDARY (713623846352979940529142984724747568191373312000M)
- WIND FARM BOUNDARY (1427247692705959881058285969449495136382746624000M)
- WIND FARM BOUNDARY (2854495385411919762116571938898990272765493248000M)
- WIND FARM BOUNDARY (5708990770823839524233143877797980545530986496000M)
- WIND FARM BOUNDARY (11417981541647679048466287755595961091061972992000M)
- WIND FARM BOUNDARY (22835963083295358096932575511191922182123945984000M)
- WIND FARM BOUNDARY (45671926166590716193865151022383844364247891968000M)
- WIND FARM BOUNDARY (91343852333181432387730302044767688728495783936000M)
- WIND FARM BOUNDARY (182687704666362864775460604089535377456991567872000M)
- WIND FARM BOUNDARY (365375409332725729550921208179070754913983135744000M)
- WIND FARM BOUNDARY (730750818665451459101842416358141509827966271488000M)
- WIND FARM BOUNDARY (1461501637330902918203684832716283019655932542976000M)
- WIND FARM BOUNDARY (2923003274661805836407369665432566039311865085952000M)
- WIND FARM BOUNDARY (5846006549323611672814739330865132078623730171904000M)
- WIND FARM BOUNDARY (11692013098647223345629478661730264157247460343808000M)
- WIND FARM BOUNDARY (23384026197294446691258957323460528314494920687616000M)
- WIND FARM BOUNDARY (46768052394588893382517914646921056628989841375232000M)
- WIND FARM BOUNDARY (93536104789177786765035829293842113257979682750464000M)
- WIND FARM BOUNDARY (187072209578355573530071658587684226515959365500928000M)
- WIND FARM BOUNDARY (374144419156711147060143317175368453031918731001856000M)
- WIND FARM BOUNDARY (748288838313422294120286634350736906063837462003712000M)
- WIND FARM BOUNDARY (1496577676626844588240573268701473812127674924007424000M)
- WIND FARM BOUNDARY (2993155353253689176481146537402947624255349848014848000M)
- WIND FARM BOUNDARY (5986310706507378352962293074805895248510699696029696000M)
- WIND FARM BOUNDARY (11972621413014756705924586149611790497021399392059392000M)
- WIND FARM BOUNDARY (23945242826029513411849172299223580994042798784118784000M)
- WIND FARM BOUNDARY (47890485652059026823698344598447161988085597568237568000M)
- WIND FARM BOUNDARY (95780971304118053647396689196894323976171195136475136000M)
- WIND FARM BOUNDARY (191561942608236107294793378393788647952342390272950272000M)
- WIND FARM BOUNDARY (383123885216472214589586756787577295904684780545900544000M)
- WIND FARM BOUNDARY (766247770432944429179173513575154591809369561091801088000M)
- WIND FARM BOUNDARY (1532495540865888858358347027150309183618739122183602176000M)
- WIND FARM BOUNDARY (3064991081731777716716694054300618367237478244367204352000M)
- WIND FARM BOUNDARY (6129982163463555433433388108601236734474956488734408704000M)
- WIND FARM BOUNDARY (12259964326927110866866776217202473468949912977468817408000M)
- WIND FARM BOUNDARY (24519928653854221733733552434404946937899825954937634816000M)
- WIND FARM BOUNDARY (49039857307708443467467104868809893875799651909875269632000M)
- WIND FARM BOUNDARY (98079714615416886934934209737619787751599303819750539264000M)
- WIND FARM BOUNDARY (196159429230833773869868419475239575503198607639501078528000M)
- WIND FARM BOUNDARY (392318858461667547739736838950479151006397215279002157056000M)
- WIND FARM BOUNDARY (784637716923335095479473677900958302012794430558004314112000M)
- WIND FARM BOUNDARY (1569275433846670190958947355801916604025588861116008628224000M)
- WIND FARM BOUNDARY (3138550867693340381917894711603833208051177722232017256448000M)
- WIND FARM BOUNDARY (6277101735386680763835789423207666416102355444464034512896000M)
- WIND FARM BOUNDARY (12554203470773361527671578846415332832204710888928069025792000M)
- WIND FARM BOUNDARY (25108406941546723055343157692830665664409421777856138051584000M)
- WIND FARM BOUNDARY (50216813883093446110686315385661331328818843555712276103168000M)
- WIND FARM BOUNDARY (100433627766186892221372631371322662657637687111424552206336000M)
- WIND FARM BOUNDARY (200867255532373784442745262742645325315275374222849104412672000M)
- WIND FARM BOUNDARY (401734511064747568885490525485290650630550748445698208825344000M)
- WIND FARM BOUNDARY (803469022129495137770981050970581301261101496891396417650688000M)
- WIND FARM BOUNDARY (1606938044258990275541962101941162602522202993782792835301376000M)
- WIND FARM BOUNDARY (3213876088517980551083924203882325205044405987565585670602752000M)
- WIND FARM BOUNDARY (6427752177035961102167848407764650410088811975131171341205504000M)
- WIND FARM BOUNDARY (12855504354071922204335696815529300820177623950262342682411008000M)
- WIND FARM BOUNDARY (25711008708143844408671393631058601640355247900524685364822016000M)
- WIND FARM BOUNDARY (51422017416287688817342787262117203280710495801049370729644032000M)
- WIND FARM BOUNDARY (102844034832575377634685574524234406561420991602098741459288064000M)
- WIND FARM BOUNDARY (205688069665150755269371149048468813122841983204197482918576128000M)
- WIND FARM BOUNDARY (411376139330301510538742298096937626245683966408394965837152256000M)
- WIND FARM BOUNDARY (822752278660603021077484596193875252491367932816789931674304512000M)
- WIND FARM BOUNDARY (1645504557321206042154969192387750504982735865633579863348609024000M)
- WIND FARM BOUNDARY (3291009114642412084309938384775501009965471731267159726697218048000M)
- WIND FARM BOUNDARY (6582018229284824168619876769551002019930943462534319453394436096000M)
- WIND FARM BOUNDARY (13164036458569648337239753539102004039861886925068638906788872192000M)
- WIND FARM BOUNDARY (26328072917139296674479507078204008079723773850137277813577744384000M)
- WIND FARM BOUNDARY (52656145834278593348959014156408016159447547700274555627155488768000M)
- WIND FARM BOUNDARY (105312291668557186697918028312816032318895095400549111254310977536000M)
- WIND FARM BOUNDARY (210624583337114373395836056625632064637790190801098222508621955072000M)
- WIND FARM BOUNDARY (421249166674228746791672113251264129275580381602196445017243910144000M)
- WIND FARM BOUNDARY (842498333348457493583344226502528258551160763204392890034487820288000M)
- WIND FARM BOUNDARY (1684996666696914987166688453005056517102321526408785780068975640576000M)
- WIND FARM BOUNDARY (3369993333393829974333376906010113034204643052817571560137951281152000M)
- WIND FARM BOUNDARY (6739986666787659948666753812020226068409286105635143120275902562304000M)
- WIND FARM BOUNDARY (13479973333575319897333507624040452136818572211270286240551805124608000M)
- WIND FARM BOUNDARY (26959946667150639794667015248080904273637144422540572481103610249216000M)
- WIND FARM BOUNDARY (53919893334301279589334030496161808547274288845081144962207220498432000M)
- WIND FARM BOUNDARY (107839786668602559178668060992323617094548577690162289924414440996864000M)
- WIND FARM BOUNDARY (215679573337205118357336121984647234189097155380324579848828881993728000M)
- WIND FARM BOUNDARY (431359146674410236714672243969294468378194310760649159697657763987456000M)
- WIND FARM BOUNDARY (862718293348820473429344487938588936756388621521298319395315527974912000M)
- WIND FARM BOUNDARY (1725436586697640946858688975877177873512777243042596638790631055949824000M)
- WIND FARM BOUNDARY (345087317339528189371737795175435574702555



C. SEABED AND SEDIMENT CLASSIFICATION CHARTS

Drawing	Chart Name	Scale
Seabed Classification Chart	GE051_TE_SBF_NU_E_10K	1 : 10,000
Sediment Classification Chart	GE051_TE_SEDIMENT_NU_10K	1 : 10,000



D. CONTACT CHARTS

Drawing	Chart Name	Scale
Contacts and Sidescan Sonar Mosaic Chart	GE051_TE_CONTACTS_NU_10K	1 : 10,000
Contacts and Magnetometer Ribbon Plot Chart	GE051_TE_RIBBON_NU_10K	1 : 10,000